

Isobar contributions to the two-nucleon interaction derived from noncovariant perturbation theory*

K. Holinde and R. Machleidt[†]

Institut für Theoretische Kernphysik der Universität Bonn, D-5300 Bonn, West Germany

M. R. Anastasio, Amand Faessler,[‡] and H. Müther

Institut für Theoretische Kernphysik der Kernforschungsanlage Jülich, D-5170 Jülich, West Germany

(Received 21 February 1978)

The fourth-order iterative diagrams involving $N\Delta$ and $\Delta\Delta$ intermediate states and including π as well as ρ exchange are calculated in momentum space without any approximation. It turns out that, due to retardation effects in the propagators, these contributions are by a factor of 3 smaller than former models using twice-iterated transition potentials with simple propagators of pion (and ρ) range. This fact allows the use of much shorter-range cutoffs at the $N\Delta$ vertices than before. NN scattering phase shifts are calculated using these diagrams together with a suitably modified one-boson exchange potential, likewise derived from noncovariant perturbation theory. The effect of the $N\Delta\rho$ vertex is different in various partial waves; its decisive role in getting a consistent description, especially of the important 3P phases, is demonstrated. It is shown that the static limit (necessarily used by other groups working in r space) is not a good approximation and, moreover, its effect cannot be mocked up by a mere change of parameters.

[NUCLEAR REACTIONS Nucleon-nucleon interaction, $NN \rightarrow N\Delta$ and $NN \rightarrow \Delta\Delta$ transition potentials with π and ρ exchange, noncovariant perturbation theory.]

I. INTRODUCTION

One of the main reasons for considering explicit isobar degrees of freedom in the two-nucleon force stems from the fact that such a procedure allows modifications of the NN interaction due to the presence of other nucleons to be taken into account. For relatively dense systems, like infinitely extended nuclear matter (and of course even more for neutron stars), it is now rather obvious that such many-body corrections play a large role.¹ Even in light nuclei, like ${}^{16}\text{O}$ (Ref. 2) and the triton,³ these modifications have nonnegligible effects.

In fact, due to new developments in the nuclear matter problem, there are good reasons to believe that the empirical saturation point cannot be obtained without including such (density dependent) modifications of the NN interaction. Recent theoretical studies of the πNN vertex function⁴ and new empirical evidence⁵ suggest a rather weak tensor force (especially a small deuteron D state probability P_D around 4%). However, usual potential models with such a low D state probability will surely overbind nuclear matter. For example, one version of the Bonn potential HM2⁶ gives about a 24 MeV binding already in a standard first-order Brueckner calculation. (The empirical binding energy is 16 MeV.) Higher-order contributions are expected to give several MeV addi-

tional attraction, i.e., even more binding. Moreover, typical variational calculations, which are nowadays more fashionable, predict overbinding even for the Reid soft-core potential,⁷ in spite of the fact that this potential has a very strong tensor force ($P_D \approx 6.4\%$). Such calculations yield ≈ 20 MeV binding compared to the 10 MeV binding predicted by a standard first-order Brueckner calculation.

Of course, for purely phenomenological models, such modifications cannot even be defined, they can only be included within a meson theoretical framework. Thus, an extended dynamical picture is necessary, not only for a basic understanding of the interaction between two nucleons, but also in order to obtain a correct description of nuclear phenomena.

The first to consider explicit $\Delta(1236)$ isobar contributions in the two-nucleon force and their quenching in nuclear matter was the group of Green and co-workers.⁸ They replaced the intermediate-range attraction of the phenomenological Reid potential⁷ in the 1S_0 partial wave by isobar contributions generated from transition potentials $V_{N\Delta}(NN \rightarrow N\Delta)$ in a coupled-channel framework. In nuclear matter, these isobar contributions are reduced due to Pauli and dispersive effects, which strongly increase with the density of the system. Thus the saturation energy is reduced by about 6 MeV, however, the density dependence of those

many-body corrections is too weak to come off the Coester line.⁸

Recently, two of the present authors⁹ have extended this method starting from a semitheoretical one-boson exchange potential.⁶ Part of the more or less fictitious σ describing the intermediate-range attraction was replaced by twice-iterated pion-range transition potentials. (It is important to note in this context that it is not realistic to replace the whole σ by Δ isobar contributions. According to what is known from the dispersion-theoretic description of 2π exchange, at least half of the intermediate-range attraction is built up by the π - π interaction). In addition to contributions arising from $NN \rightarrow N\Delta$, those arising from the transition $NN \rightarrow \Delta\Delta$ were also taken into account. Furthermore, the isobar contributions were consistently included in all partial waves and an accurate fit of all NN scattering phase shifts and deuteron data was obtained. A standard first-order nuclear matter calculation moved the saturation energy of HM2⁶ from -24 MeV to about -10 MeV.

In these calculations, however, an artificially strong cutoff was required to prevent a Δ contribution larger than half of the total σ contribution. Consequently, the results show a strong sensitivity to the cutoff parameter. This effect can be partly traced back to the neglect of ρ exchange at the $N\Delta$ vertex. At least in S states, it cancels part of the pion-range transition potentials and thus should weaken the cutoff dependence. In fact, according to preliminary calculations,¹⁰ the consideration of ρ exchange not only reduces the cutoff dependence, but also removes characteristic discrepancies in higher partial-wave phase shifts ($L \geq 1$).

It has become a matter of controversy whether the simple pion-range propagator $(\vec{\Delta}^2 + m_\pi^2)^{-1}$, ($\vec{\Delta}$ being the momentum transfer) can provide a realistic description. The transition potential concept can handle without difficulties only those time-ordered diagrams which have a pure baryonic intermediate state (iterative diagrams), i.e., only the first 4 out of 12 (if antiparticles are neglected) as shown in Fig. 1. According to Smith and Pandharipande,¹¹ the pion-range propagator might summarize the effect of all 12 diagrams to a certain approximation. However, their arguments rely heavily on cancellations between crossed-box diagrams (involving NN , $N\Delta$, and $\Delta\Delta$ states). These critically depend on the detailed structure of the πNN and $\pi N\Delta$ vertices which are not known to a sufficient accuracy. Moreover, it is not clear whether these cancellations persist in higher orders.

Since most people dealing with isobar contributions work in coordinate space, it is clear why so

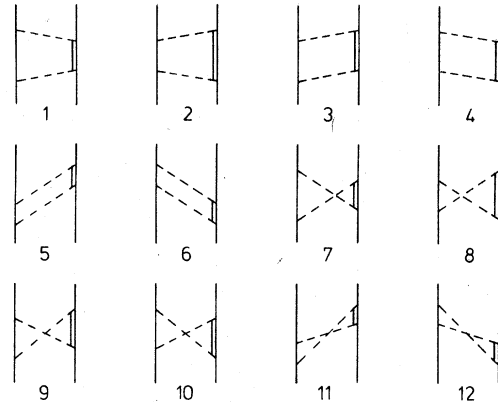


FIG. 1. Time-ordered diagrams with positive energy $N\Delta$ intermediate states.

much effort is put into avoiding the exact time-ordered propagators. The reason is simply that these propagators (defined in momentum space) cannot be transformed analytically into r space. They can only be handled approximately, simulating them by manageable r space expressions. This is very cumbersome, see e.g., the recent work of Saarela.¹²

In our case, however, these time-ordered propagators present no problem since we work throughout in momentum space, see Ref. 9. Furthermore, as shown by Schütte,¹³ the use of time-ordered perturbation theory provides a unified scheme for the two-body as well as the many-body problem, i.e., the transition from the two-body to the many-body problem is well defined. In fact, this scheme already defines modifications of the NN interaction in the medium for the pure one-boson exchange (OBE) picture (without introducing isobars). According to calculations done by Kotthoff *et al.*,¹⁴ the OBE potential (mainly the pion-exchange part) is quenched in the medium, which reduces the saturation energy in nuclear matter by about 5 MeV.

There is another reason why time-ordered propagators should be used instead of the simple pion-range propagator. Recent dispersion-theoretical investigations¹⁵ have shown that the use of the pion-range propagator overestimates the isobar contribution by a factor of 2 or 3. The use of exact time-ordered propagators reduces the isobar contributions (as will become clear later, see also Ref. 12) and are thus more in line with dispersion theory.

One may ask why not use the results of dispersion theory directly in order to construct a nucleon-nucleon potential. Then all diagrams like those of Fig. 1 are automatically included in the right way, and one avoids all the difficulties with

explicit field-theoretical models. In fact, if we would restrict our considerations to the two-nucleon problem, dispersion theory is probably the best one can do since it provides strong constraints due to correlations with πN and $\pi\pi$ scattering data. However, if the final aim is to understand nuclear-structure phenomena, we strongly believe that modifications of the NN interaction have to be taken into account. These cannot be handled in a dispersion-theoretical treatment. Of course, the results of dispersion theory should be used as a constraint for explicit field-theoretical models in order to pin down ambiguities in propagators, form factors, and so on.

In this paper, it is our aim to present a detailed study (a) of the $N\Delta\rho$ vertex and (b) of the exact time-ordered propagators, i.e., we calculate the first four diagrams in Fig. 1, including $(\pi + \rho)$ exchange. It will turn out that both effects reduce strongly the isobar contribution with pion range found in Ref. 9. This will allow cutoff parameters at the $N\Delta\pi$ vertices which are in a much more reasonable range than before, i.e., like in the other OBE vertices. Furthermore, since our calculations are carried out in momentum space, we are able to take into account the full complexity of the $N\Delta$ vertex functions. Therefore, we can study the approximation of going to the static limit at the $N\Delta$ vertices, which has to be used by other authors in order to obtain manageable r space expressions.

II. OUTLINE OF THE FORMALISM

In this chapter we evaluate explicitly the first four (iterative) diagrams of Fig. 1, which can be

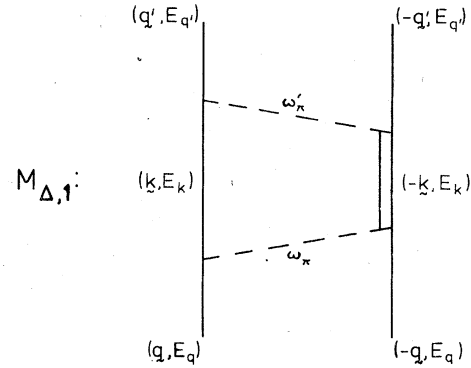


FIG. 2. Notation for the first diagram in Fig. 1.

reproduced by iteration of a transition potential. In addition, we also evaluate the four similar diagrams with two isobars in the intermediate states.

We first consider the case of π exchange and start with the usual interaction Lagrangians

$$L_{NN\pi} = \sqrt{4\pi} g_\pi i \bar{\Psi} \vec{\tau} \gamma^5 \Psi \vec{\phi}, \quad (2.1)$$

$$L_{N\Delta\pi} = \sqrt{4\pi} \frac{f_{N\Delta\pi}}{m_\pi} \bar{\Psi} \vec{T} \Psi^\mu \partial_\mu \vec{\phi} + \text{H.c.},$$

where g_π is the pion-nucleon coupling constant, $f_{N\Delta\pi}$ the coupling constant at the $N\Delta$ vertex, and m_π is the pion mass. Here Ψ denotes the nucleon field operator, ϕ the pion field, Ψ^μ the field operator of the Δ isobar and τ, T are isospin matrices. According to standard rules (see Refs. 13 and 14), the first diagram of Fig. 1, which for convenience is redrawn in Fig. 2, can be generated by the second iteration of a transition potential $V_{N\Delta,1}$, namely,

$$\langle \bar{q}' \Lambda'_1 \Lambda'_2 | M_{N\Delta,1}^\pi(z) | \bar{q} \Lambda_1 \Lambda_2 \rangle = \sum_{h_1, h_2^*} \int d^3k \frac{\langle \bar{q}' \Lambda'_1 \Lambda'_2 | V_{N\Delta,1}^\pi(z) | \bar{k} h_1 h_2^* \rangle \langle \bar{k} h_1 h_2^* | V_{N\Delta,1}^\pi(z) | \bar{q} \Lambda_1 \Lambda_2 \rangle}{E_k^* + E_k - z}, \quad (2.2)$$

with

$$\langle \bar{q}' \Lambda'_1 \Lambda'_2 | V_{N\Delta,1}^\pi(z) | \bar{q} \Lambda_1 \Lambda_2 \rangle = \frac{4\pi}{(2\pi)^3} \frac{g_\pi f_{N\Delta\pi}}{m_\pi} \frac{M}{E_{q'}} \left(\frac{MM_\Delta}{E_q E_q^*} \right)^{1/2} \vec{\tau}_1 \cdot \vec{T}_2 F_\pi(q', q) \Delta_\mu \frac{\bar{u}_{\Lambda_2}(-\vec{q}') u_{\Lambda_2}^*(-\vec{q}) \bar{u}_{\Lambda_1}(\vec{q}') \gamma^5 u_{\Lambda_1}(\vec{q})}{2\omega_\pi(E_{q'} + E_q + \omega_\pi - z)}, \quad (2.3)$$

where $E_q = (M^2 + \vec{q}^2)^{1/2}$, $E_q^* = (M_\Delta^2 + \vec{q}^2)^{1/2}$, M is the mass of the nucleon ($= 938.9$ MeV), and M_Δ is the mass of the Δ isobar ($= 1236$ MeV). Also, z is the starting energy, ω_π is the energy of the exchanged pion, $\omega_\pi = [(\vec{q}' - \vec{q})^2 + m_\pi^2]^{1/2}$, and $\Delta_\mu = (q' - q)_\mu$. The

summation goes over the helicities of the particles in the intermediate states, i.e., $h_1 = \pm \frac{1}{2}$, $h_2^* = \pm \frac{1}{2}, \pm \frac{3}{2}$, since the Δ isobar has spin $\frac{3}{2}$. Here, u denotes the Dirac spinor describing the nucleon, whereas u^μ is the conventional Rarita-Schwinger spinor

describing the isobar. F_π is a dipole-type cutoff

$$F_\pi = \left(\frac{\Lambda_\pi^2 - m_\pi^2}{\Lambda_\pi^2 + (\vec{q}' - \vec{q})^2} \right)^2, \quad (2.4)$$

with Λ_π a parameter, the so called cutoff mass.

The sum of diagrams 1-4 of Fig. 1 plus those in which the Δ appears on the left-hand side, can then be written as

$$\langle \vec{q}' \Lambda'_1 \Lambda'_2 | M_{N\Delta}^\pi(z) | \vec{q} \Lambda_1 \Lambda_2 \rangle = \sum_{h_1^*, h_2^*} \int d^3k \frac{\langle \vec{q}' \Lambda'_1 \Lambda'_2 | V_{N\Delta}^\pi(z) | \vec{k} h_1 h_2^* \rangle \langle \vec{k} h_1 h_2^* | V_{N\Delta}^\pi(z) | \vec{q} \Lambda_1 \Lambda_2 \rangle}{E_k^* + E_k - z}, \quad (2.5)$$

with

$$V_{N\Delta}^\pi = (V_{N\Delta,1}^\pi + V_{N\Delta,2}^\pi) \sqrt{2}. \quad (2.6)$$

$V_{N\Delta,2}^\pi$ differs from Eq. (2.3) only in the denominator, where E_q has to be replaced by E_q^* .

Analogously, the sum of the iterative diagrams involving $\Delta\Delta$ intermediate states is given by

$$\langle \vec{q}' \Lambda'_1 \Lambda'_2 | M_{\Delta\Delta}^\pi(z) | \vec{q} \Lambda_1 \Lambda_2 \rangle = \sum_{h_1^*, h_2^*} \int d^3k \frac{\langle \vec{q}' \Lambda'_1 \Lambda'_2 | V_{\Delta\Delta}^\pi(z) | \vec{k} h_1^* h_2^* \rangle \langle \vec{k} h_1^* h_2^* | V_{\Delta\Delta}^\pi(z) | \vec{q} \Lambda_1 \Lambda_2 \rangle}{2E_k^* - z}, \quad (2.7)$$

with

$$V_{\Delta\Delta}^\pi = V_{\Delta\Delta,1}^\pi + V_{\Delta\Delta,2}^\pi, \quad (2.8)$$

where

$$\langle \vec{q}' \Lambda'_1 \Lambda'_2 | V_{\Delta\Delta,1}^\pi(z) | \vec{q} \Lambda_1 \Lambda_2 \rangle = \frac{4\pi}{(2\pi)^3} \frac{f_{N\Delta\pi^2}}{m_\pi^2} \frac{MM_\Delta}{E_{q'} E_q^*} \vec{T}_1 \cdot \vec{T}_2 F_\pi(\vec{q}', \vec{q}) \Delta_\mu \Delta_\nu \frac{\bar{u}_{\Lambda'_2}(-\vec{q}') u_{\Lambda'_2}^*(-\vec{q}) \bar{u}_{\Lambda_1}(\vec{q}') u_{\Lambda_1}^*(\vec{q})}{2\omega_\pi(E_{q'} + E_q^* + \omega_\pi - z)} \quad (2.9)$$

and $V_{\Delta\Delta,2}^\pi$ is the same as $V_{\Delta\Delta,1}^\pi$. Explicit expressions for $V_{N\Delta}^\pi$ and $V_{\Delta\Delta}^\pi$ can be found in the appendix of Ref. 9. Only the denominators have to be changed appropriately. [Note also that the denominators are the same if one neglects retardation effects in Eqs. (2.3) and (2.9).]

Next we evaluate the contribution from ρ exchange. We start from the interaction Lagrangians

$$L_{NN\rho} = \sqrt{4\pi} \left(g_\rho \bar{\Psi} \gamma_\alpha \vec{T} \Psi \vec{\phi}^\alpha + \frac{f_\rho}{4M} \bar{\Psi} \sigma^{\mu\nu} \vec{T} \Psi (\partial_\mu \vec{\phi}_\nu - \partial_\nu \vec{\phi}_\mu) \right), \quad (2.10)$$

$$L_{N\Delta\rho} = \sqrt{4\pi} i \frac{f_{N\Delta\rho}}{m_\rho} \bar{\Psi} \gamma^5 \gamma^\mu \vec{T} \Psi^\nu (\partial_\mu \vec{\phi}_\nu - \partial_\nu \vec{\phi}_\mu),$$

where g_ρ, f_ρ are respectively, the vector and tensor ρNN coupling constants, $f_{N\Delta\rho}$ is the $N\Delta\rho$ coupling, and m_ρ is the mass of the ρ meson; $\sigma^{\mu\nu} = \frac{1}{2} i [\gamma^\mu, \gamma^\nu]$.

Thus we obtain for the first four diagrams of Fig. 1 (plus those where the Δ appears on the left-hand side) with ρ exchange

$$\langle \vec{q}' \Lambda'_1 \Lambda'_2 | M_{N\Delta}^\rho(z) | \vec{q} \Lambda_1 \Lambda_2 \rangle = \sum_{h_1^*, h_2^*} \int d^3k \frac{\langle \vec{q}' \Lambda'_1 \Lambda'_2 | V_{N\Delta}^\rho(z) | \vec{k} h_1 h_2^* \rangle \langle \vec{k} h_1 h_2^* | V_{N\Delta}^\rho(z) | \vec{q} \Lambda_1 \Lambda_2 \rangle}{E_k^* + E_k - z}, \quad (2.11)$$

with

$$V_{N\Delta}^\rho = (V_{N\Delta,1}^\rho + V_{N\Delta,2}^\rho) \sqrt{2}, \quad (2.12)$$

where

$$\begin{aligned} \langle \vec{q}' \Lambda'_1 \Lambda'_2 | V_{N\Delta,1}^\rho(z) | \vec{q} \Lambda_1 \Lambda_2 \rangle &= \frac{4\pi}{(2\pi)^3} \frac{f_{N\Delta\rho}}{m_\rho} \frac{M}{E_{q'}} \left(\frac{MM_\Delta}{E_q E_q^*} \right)^{1/2} \vec{T}_1 \cdot \vec{T}_2 F_\rho(\vec{q}', \vec{q}) \bar{u}_{\Lambda'_2}(-\vec{q}') \gamma^5 \gamma^\mu \mu_{\Lambda_2}^*(\vec{q}) \\ &\times \frac{g_\nu^\beta \Delta_\mu - g_\mu^\beta \Delta_\nu}{2\omega_\rho(E_{q'} + E_q + \omega_\rho - z)} \bar{u}_{\Lambda'_1}(\vec{q}') \left(g_\rho \gamma_\beta + \frac{f_\rho}{2M} i \sigma_{\beta\alpha} \Delta^\alpha \right) u_{\Lambda_1}(\vec{q}) \end{aligned} \quad (2.13)$$

and again, $V_{N\Delta,2}^\rho$ differs from $V_{N\Delta,1}^\rho$ only in the denominator, where E_q has to be replaced by E_q^* . Correspondingly,

$$\langle \vec{q}' \Lambda'_1 \Lambda'_2 | M_{\Delta\Delta}^\rho(z) | \vec{q} \Lambda_1 \Lambda_2 \rangle = \sum_{h_1^*, h_2^*} \int d^3k \frac{\langle \vec{q}' \Lambda'_1 \Lambda'_2 | V_{\Delta\Delta}^\rho(z) | \vec{k} h_1^* h_2^* \rangle \langle \vec{k} h_1^* h_2^* | V_{\Delta\Delta}^\rho(z) | \vec{q} \Lambda_1 \Lambda_2 \rangle}{2E_k^* - z}, \quad (2.14)$$

with

$$V_{\Delta\Delta}^{\rho} = V_{\Delta\Delta,1}^{\rho} + V_{\Delta\Delta,2}^{\rho}, \quad (2.15)$$

where

$$\begin{aligned} \langle \bar{q}' \Lambda_1' \Lambda_2' | V_{\Delta\Delta,1}^{\rho}(z) | \bar{q} \Lambda_1^* \Lambda_2^* \rangle &= \frac{4\pi}{(2\pi)^3} \frac{f_{N\Delta\rho}^2}{m_{\rho}^2} \frac{MM_{\Delta}}{E_q' E_q^*} \bar{T}_1 \cdot \bar{T}_2 F_{\rho}(\bar{q}', \bar{q}) \bar{u}_{\Lambda_2'}(-\bar{q}) \gamma^5 \gamma^{\mu} u_{\Lambda_2^*}^{\nu}(-\bar{q}) u_{\Lambda_1'}(\bar{q}') \gamma^5 \gamma^{\alpha} u_{\Lambda_1^*}^{\beta}(\bar{q}) \\ &\times \frac{\Delta_{\mu} \Delta_{\alpha} g_{\beta\nu} - \Delta_{\mu} \Delta_{\beta} g_{\nu\alpha} - \Delta_{\nu} \Delta_{\alpha} g_{\mu\beta} + \Delta_{\nu} \Delta_{\beta} g_{\alpha\mu}}{2\omega_{\rho}(E_q' + E_q^* + \omega_{\rho} - z)} \end{aligned} \quad (2.16)$$

and $V_{\Delta\Delta,2}^{\rho}$ is the same as $V_{\Delta\Delta,1}^{\rho}$. The form factor is chosen to be

$$F_{\rho} = \left(\frac{\Lambda_{\rho}^2 - m_{\rho}^2}{\Lambda_{\rho}^2 + (\bar{q}' - \bar{q})^2} \right)^3, \quad (2.17)$$

with Λ_{ρ} being a cutoff parameter. For convenience, we give explicit results for specific matrix elements of $V_{N\Delta}^{\rho}$ and $V_{\Delta\Delta}^{\rho}$ in the appendix.

The sum of all possible exchanges in diagrams 1–4 of Fig. 1 (including those with mixed π, ρ exchange) can then be written as

$$\begin{aligned} \langle \bar{q}' \Lambda_1' \Lambda_2' | M_{N\Delta}(z) | \bar{q} \Lambda_1 \Lambda_2 \rangle &= \sum_{h_1^*, h_2^*} \int \frac{d^3k}{E_k^* + E_k - z} [\langle \bar{q}' \Lambda_1' \Lambda_2' | V_{N\Delta}^{\pi}(z) | \bar{k} h_1 h_2^* \rangle + \langle \bar{q}' \Lambda_1' \Lambda_2' | V_{N\Delta}^{\rho}(z) | \bar{k} h_1 h_2^* \rangle] \\ &\times [\langle \bar{k} h_1 h_2^* | V_{N\Delta}^{\pi}(z) | \bar{q} \Lambda_1 \Lambda_2 \rangle + \langle \bar{k} h_1 h_2^* | V_{N\Delta}^{\rho}(z) | \bar{q} \Lambda_1 \Lambda_2 \rangle] \end{aligned} \quad (2.18)$$

and for $\Delta\Delta$ intermediate states

$$\begin{aligned} \langle \bar{q}' \Lambda_1' \Lambda_2' | M_{\Delta\Delta}(z) | \bar{q} \Lambda_1 \Lambda_2 \rangle &= \sum_{h_1^*, h_2^*} \int \frac{d^3k}{2E_k^* - z} [\langle \bar{q}' \Lambda_1' \Lambda_2' | V_{\Delta\Delta}^{\pi}(z) | \bar{k} h_1^* h_2^* \rangle + \langle \bar{q}' \Lambda_1' \Lambda_2' | V_{\Delta\Delta}^{\rho}(z) | \bar{k} h_1^* h_2^* \rangle] \\ &\times [\langle \bar{k} h_1^* h_2^* | V_{\Delta\Delta}^{\pi}(z) | \bar{q} \Lambda_1 \Lambda_2 \rangle + \langle \bar{k} h_1^* h_2^* | V_{\Delta\Delta}^{\rho}(z) | \bar{q} \Lambda_1 \Lambda_2 \rangle]. \end{aligned} \quad (2.19)$$

One final remark should be made. Of course, these iterative diagrams could have been obtained without introducing the concept of transition potentials. Specifically, the sum over intermediate helicities can be replaced by suitable projection operators. However, transition potentials are explicitly needed in order to calculate isobar components of wave functions, which are of considerable importance in nuclear physics. (We will, however, not perform such calculations in this paper.) It should also be noted that in order to make the cutoff mass in F_{π} equivalent to the one used in Ref. 9, we have multiplied both F_{π} and F_{ρ} in Eqs. (2.4) and (2.17) by the factor $(E_q^* M / E_q M_{\Delta})^{1/2}$ in the definition of $V_{N\Delta}$ and by $E_q^* M / E_q M_{\Delta}$ in the definition of $V_{\Delta\Delta}$.

In order to calculate phase shifts, we define an effective potential

$$V_{\text{eff}}(z) = V_{\text{OBE}}(z) - M_{N\Delta}(z) - M_{\Delta\Delta}(z). \quad (2.20)$$

Here, $V_{\text{OBE}}(z)$ is the one-boson-exchange potential of Ref. 14 with suitably modified parameters. In contrast to Ref. 14, we now make a more convenient choice for the form factors, i.e., in V_{OBE} we choose

$$F_{\alpha} = \left(\frac{\Lambda_{\alpha}^2 - m_{\alpha}^2}{\Lambda_{\alpha}^2 - \Delta^2} \right)^n \quad (2.21)$$

at the vertices, with $n=1$ for $\alpha = \pi, \eta, \sigma, \delta$ and $n = \frac{3}{2}$ for $\alpha = \rho, \omega, \phi$; $\Delta^2 = (E_q' - E_q)^2 - (\bar{q}' - \bar{q})^2$. $M_{\Delta\Delta}(z)$ and $M_{N\Delta}(z)$ are obtained from Eqs. (2.18) and (2.19). The R matrix is then given by

$$R(z) = V_{\text{eff}}(z) + V_{\text{eff}}(z) \frac{P}{z - H_0} R(z), \quad (2.22)$$

where P denotes the principal value. Explicitly, we obtain, in partial waves and helicity state basis,

$$\begin{aligned} &\langle \Lambda_1' \Lambda_2' | R^J(q', q | z) | \Lambda_1 \Lambda_2 \rangle \\ &= \langle \Lambda_1' \Lambda_2' | V_{\text{eff}}^J(q', q | z) | \Lambda_1 \Lambda_2 \rangle \\ &- \sum_{h_1, h_2} P \int_0^{\infty} \frac{dk k^2}{2E_k - z} \langle \Lambda_1' \Lambda_2' | V_{\text{eff}}^J(q', k | z) | h_1 h_2 \rangle \\ &\quad \times \langle h_1 h_2 | R^J(q', q | z) | \Lambda_1 \Lambda_2 \rangle. \end{aligned} \quad (2.23)$$

Here, the starting energy is $z = 2E_q$. The deuteron data are calculated analogously. For further details, we refer to Refs. 9 and 14 and to the review article of Erkelenz.¹⁶

TABLE I. Parameters for the transition potentials. Here Λ_π and Λ_ρ are given in MeV.

$f_{N\Delta\pi}^2$	$f_{N\Delta\rho}^2$	Λ_π	Λ_ρ
0.27	15.41	1200	1200

III. RESULTS AND DISCUSSION

The parameters in the transition potentials, used throughout this paper, are given in Table I. The value 0.27 for $f_{N\Delta\pi}^2$ is between the Chew-Low value (0.32) and the value derived from the quark model (0.23) and is actually suggested from πN studies.¹⁷ $f_{N\Delta\rho}^2$ is obtained using the usual relation¹ based on the quark model

$$f_{N\Delta\rho}^2 = \frac{f_{N\Delta\pi}^2}{f_\pi^2} g_\rho^2 \frac{m_\rho^2}{4M^2} (1 + f_\rho/g_\rho)^2,$$

where $f_\pi^2 = (m_\pi/2M)^2 g_\pi^2$, $g_\pi^2 = 14.4$, and $g_\rho^2 = 0.55$, $f_\rho/g_\rho = 6.6$ as suggested by the analysis of Höhler

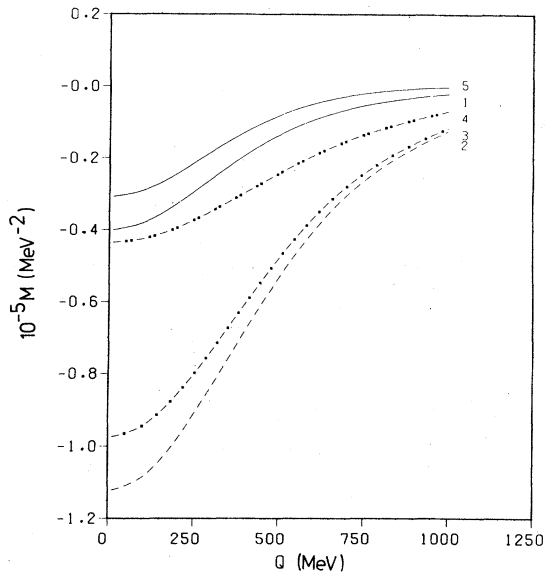


FIG. 3. The $N\Delta$ contribution with only π exchange, i.e., the contribution of $\langle q' | M_{N\Delta}^\pi(z) | q \rangle$ in Eq. (2.5), for the 1S_0 partial wave, with $q' = q_0 = 250$ MeV [$z = 2(q_0^2 + M^2)^{1/2}$] as a function of q is denoted by the solid lines. Curve 1 shows the full relativistic results while curve 5 shows the results when the static limit is taken at the $N\Delta$ vertices. The dashed curve (curve 2) is obtained by replacing the time-ordered propagators in the transition potentials $V_{N\Delta,1}^\pi$ and $V_{N\Delta,2}^\pi$ by simple pion-range propagators. The dashed-dot curve (curve 3) is obtained using the prescription of Durso *et al.* (Ref. 15), i.e., taking $V_{N\Delta,1}^\pi$ as in curve 2 but using a range of $\sqrt{3}m_\pi$ in $V_{N\Delta,2}^\pi$. In the dashed double-dot curve (curve 4) the range in $V_{N\Delta,1}^\pi$ is taken as $2m_\pi$, while it is taken as $4m_\pi$ in $V_{N\Delta,2}^\pi$.

and Pietarinen.¹⁸ The cutoff parameters are chosen to be 1200 MeV in both F_π and F_ρ and are therefore in a much more reasonable range than before.⁹

In Fig. 3 (solid line) we show the contribution of diagrams 1–4 of Fig. 1 (plus those in which the Δ appears on the left-hand side) involving only π exchange, i.e., the contribution of Eq. (2.5), in the 1S_0 partial wave, for $q' = q_0 = 250$ MeV [$z = 2(q_0^2 + M^2)^{1/2}$]. The dashed line is obtained by replacing the time-ordered propagators in both $V_{N\Delta,1}^\pi$ and $V_{N\Delta,2}^\pi$ by simple pion-range propagators, i.e., by $(\vec{q}' - \vec{q})^2 + m_\pi^2$; in other words, retardation effects are neglected. It is seen that these retardation effects suppress the contribution by a factor of 3. In Ref. 15, a modification of the pion-range propagator, still tractable in r space, was proposed in order to take into account these effects. It consists of taking $V_{N\Delta,1}^\pi$ the same as before, but using for the propagator in $V_{N\Delta,2}^\pi$ $(\vec{q}' - \vec{q})^2 + 3m_\pi^2$, i.e., the range is shortened to $\sqrt{3}m_\pi$. We see that the result (dash-dot line) goes in the right direction, however, the effect is only 20% of the total retardation effect. That this modification underestimates the effect can be traced back to severe approximations used to derive it (initial nucleons at rest and neglect of nucleon recoil effects), as was already recognized in Ref. 15.

This shows that, in order to simulate the exact time-ordered propagator, the range has to be chosen much shorter. We arbitrarily chose $2m_\pi$ for $V_{N\Delta,1}^\pi$ [i.e., $(\vec{q}' - \vec{q})^2 + 4m_\pi^2$ for the propagator] and $4m_\pi$ for $V_{N\Delta,2}^\pi$. The result is given by the dash-double dot curve. It is seen that this (phenomenological) prescription roughly agrees with the correct result for low momenta q , but overestimates it for higher q . This suggests that a very sophisticated prescription is needed in order to replace time-ordered propagators by manageable r space expressions, see also Ref. 12. In any case, such a replacement destroys the specific structure of the propagator necessary for a well defined prescription in going from two-body scattering to nuclear structure, see Ref. 13.

In addition, we show the results if we go to the static limit at the $N\Delta$ vertices in Eq. (2.5), keeping the propagators the same. It reduces the exact contribution by roughly 25%. Our calculations have shown that this is true for all propagators considered in this figure. Thus the combined use of (i) the static limit at the vertices and (ii) the pion-range propagator (as is usually done in r space calculations, see Ref. 1) overestimates the contribution from an exact calculation of diagrams 1–4 by roughly a factor of 2.

Figure 4 shows the corresponding results for the contribution of the iterative diagrams involv-

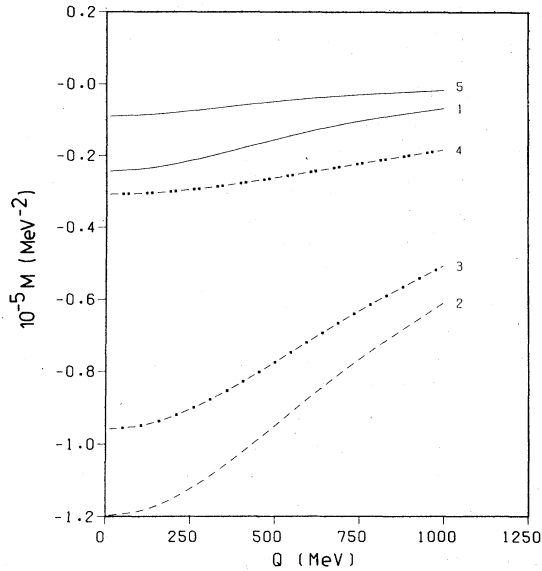


FIG. 4. The results for the $\Delta\Delta$ contribution with only π exchange, i.e., Eq. (2.7), with the same notation as in Fig. 3. For the Durso *et al.* (Ref. 15) prescription (curve 3), both $V_{\Delta\Delta,1}^\pi$ and $V_{\Delta\Delta,2}^\pi$ have range $\sqrt{3}m_\pi$, while for curve 4 they both have range $4m_\pi$.

ing $\Delta\Delta$ intermediate states, i.e., the contribution of Eq. (2.7). The modifications of the range are, however, consistently changed compared to the former case: for the dash-dot line, m_π is now replaced by $\sqrt{3}m_\pi$ in the propagators of both $V_{\Delta\Delta,1}^\pi$ and $V_{\Delta\Delta,2}^\pi$; for the dash-double dot line, m_π is replaced by $4m_\pi$ both in $V_{\Delta\Delta,1}^\pi$ and $V_{\Delta\Delta,2}^\pi$. There are characteristic differences compared to Fig. 3. First, the relative contribution of higher momenta is much larger now; this shows that the $\Delta\Delta$ contribution is considerably shorter ranged than the $N\Delta$ contribution of Fig. 3. Second, for low momenta, the $N\Delta$ and $\Delta\Delta$ contributions are roughly the same for the pion-range propagator, whereas the use of the exact time-ordered propagators reduces the $\Delta\Delta$ contribution relative to the $N\Delta$ contribution. On the other hand, the effect of modifying the range is the same as in Fig. 3. Also, the use of the static limit at the vertices together with the pion-range propagator overestimates the true contribution again by roughly a factor of 2.

A comparison with Fig. 2 of Ref. 9 shows that, for lower momenta, the sum of the $N\Delta$ and $\Delta\Delta$ contribution, i.e., the sum of Eq. (2.5) and (2.7), agrees roughly with the corresponding contribution using the pion-range propagator and $\Lambda_\pi \sim 850$ MeV (the different values for $f_{N\Delta\pi}^2$ used in this work and in Ref. 9 have to be taken into account). In other words, the use of the exact time-ordered propagators allows the use of $\Lambda_\pi = 1200$ MeV in-

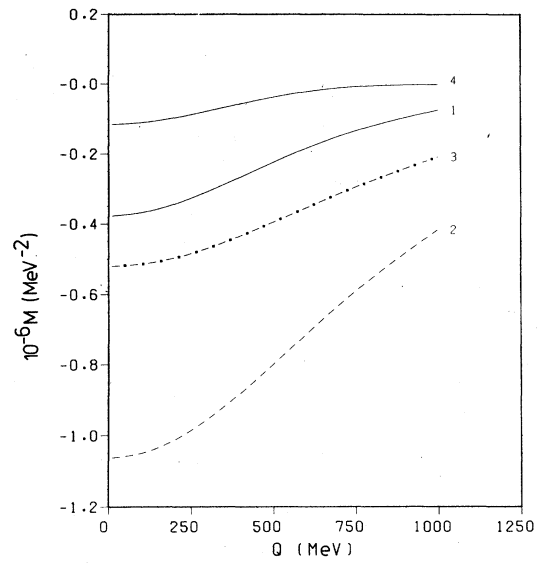


FIG. 5. The analogous $N\Delta$ contribution to Fig. 3 for only ρ exchange. Again the solid curves denote the results for the full relativistic and static limit cases, curves 1 and 4, respectively. Curve 2 denotes the results with simple ρ -range propagators in $V_{N\Delta,1}^\rho$ and $V_{N\Delta,2}^\rho$ while for curve 3, when the Durso *et al.* (Ref. 15) prescription is used, m_ρ^2 is replaced by $m_\rho^2 + m_\rho(M_\Delta - M)$ in the propagator for $V_{N\Delta,2}^\rho$.

stead of $\Lambda_\pi = 850$ MeV.

In Figs. 5 and 6, we show the analogous contributions for ρ exchange, i.e., Eqs. (2.11) and (2.14). Again, the exact time-ordered propagators reduce the contribution obtained with the usual choice [i.e., $(q' - q)^2 + m_\rho^2$ as propagator] by roughly a factor of 3 as in the case of pion exchange. This shows that the effect of time-ordered propagators cannot be neglected as suggested in Ref. 12. The dash-dot line again shows the result for a modification of the ρ range propagator according to Ref. 15. In Fig. 5, m_ρ^2 is replaced by $m_\rho^{*2} \approx m_\rho^2 + m_\rho(M_\Delta - M)$ in the propagator of $V_{N\Delta,2}^\rho$ ($V_{N\Delta,1}^\rho$ is the same as for the dashed line); in Fig. 6, m_ρ^2 is replaced by m_ρ^{*2} in the propagator of both $V_{N\Delta,1}^\rho$ and $V_{N\Delta,2}^\rho$. We see that the agreement with the exact result is much better than for the pion case. Again, the combined use of the static limit at the vertices and ρ range propagator [$[(\vec{q}' - \vec{q})^2 + m_\rho^2]$] overestimates the exact result by roughly a factor of 2.

The next two figures show the effect of combining the π and ρ exchange contributions. In Fig. 7, the two dashed lines show the $N\Delta$ contribution, i.e., $M_{N\Delta}(z)$ of Eq. (2.18), again in the 1S_0 partial wave for $q' = q_0 = 250$ MeV. Curve 3 denotes the full (relativistic) result, whereas curve 4 shows the result if the static limit is taken at the $N\Delta$

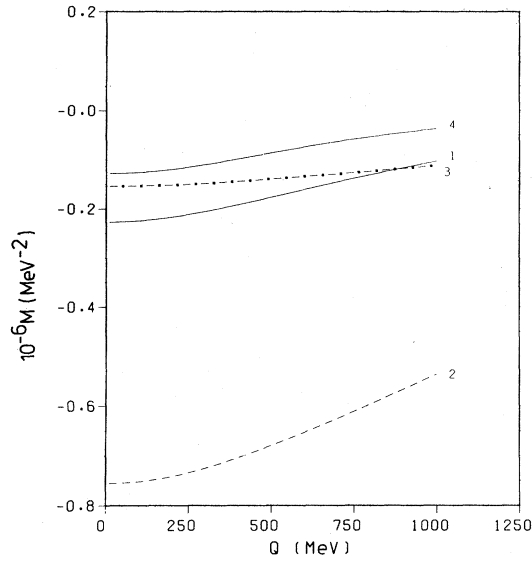


FIG. 6. The analogous $\Delta\Delta$ contribution to Fig. 4 for only ρ exchange. The notation is the same as in Fig. 5 except for curve 3, where m_ρ^2 is replaced by $m_\rho^2 + m_\rho(M_\Delta - M)$ in the propagators of both $V_{\Delta\Delta,1}^\rho$ and $V_{\Delta\Delta,2}^\rho$.

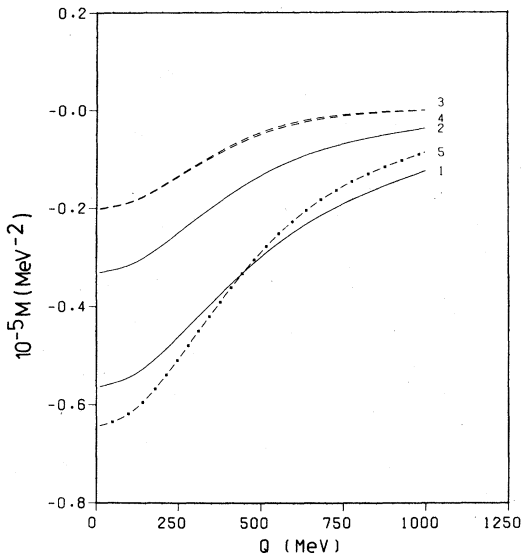


FIG. 7. Results from combining π and ρ exchange using time-ordered propagators. The solid curves denote the $N\Delta$ and $\Delta\Delta$ contributions with π and ρ exchange, i.e., $M_{N\Delta} + M_{\Delta\Delta}$. The dashed curves denote only the $N\Delta$ contribution with π and ρ exchange, i.e., $M_{N\Delta}$. Both the full relativistic and static limit cases are shown, curves 1 and 3 and curves 2 and 4, respectively. The $N\Delta$ and $\Delta\Delta$ contribution with only π exchange is also given by the dashed-dot curve. As before, the results are shown for the 1S_0 partial wave with $q' = q_0 = 250$ MeV.

vertices. A comparison with Fig. 3 shows that the inclusion of ρ exchange suppresses the $N\Delta$ contribution by a factor of 2 in this partial wave. The result for the static limit happens to be the same in spite of the fact that both π and ρ contributions are strongly modified separately. This feature, however, does not persist in higher partial waves.

The two solid curves (curves 1 and 2) denote the sum of $N\Delta$ and $\Delta\Delta$ contributions, for the relativistic case and the static limit, respectively, i.e., the sum of Eqs. (2.18) and (2.19). Thus the difference between curves 1 and 3 or between curves 2 and 4 gives the $\Delta\Delta$ contribution. A comparison with Fig. 4 shows that the $\Delta\Delta(\pi + \rho)$ contribution is in fact larger than the $\Delta\Delta, \pi$ contribution, i.e., in this channel, the inclusion of ρ exchange enlarges the $\Delta\Delta$ contribution. The strong reduction of the total contribution due to the static limit (nearly by a factor of 2) can be completely traced back to the reduction of the $\Delta\Delta$ contribution. The dash-dot curve shows only the π contribution ($N\Delta + \Delta\Delta$), which roughly agrees with the corresponding $(\pi + \rho)$ contribution. Again, the strong reduction of the $N\Delta, \pi$ contribution by adding ρ exchange is partly cancelled by an increase of $\Delta\Delta, \pi$ due to the inclusion of ρ exchange.

In Fig. 8, the two solid lines (curves 1 and 2)

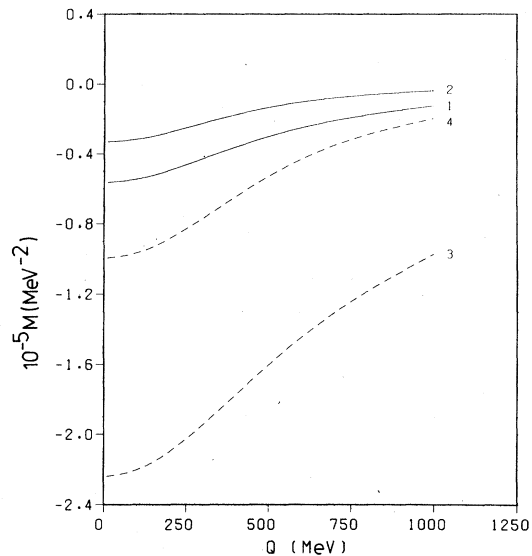


FIG. 8. Results from combining π and ρ exchange using simple π - and ρ -range propagators. The dashed curves denote the $N\Delta$ and $\Delta\Delta$ contribution with π and ρ exchange replacing the time-ordered propagators in the transition potentials by simple π - and ρ -range propagators. The solid curves denote the same results with time-ordered propagators. Both the full relativistic and static limit cases are shown, curves 1 and 3 and curves 2 and 4, respectively.

again show the ($N\Delta + \Delta\Delta$) contribution arising from ($\pi + \rho$) exchange. The two dashed lines (curves 3 and 4) show the results when the time-ordered propagators in the transition potentials are replaced by usual pion-range and ρ -range propagators [i.e., $(\vec{q}' - \vec{q})^2 + m_\pi^2$, $(\vec{q}' - \vec{q})^2 + m_\rho^2$]. As before, curves 1 and 3 show the relativistic result and curves 2 and 4 the static limit at the $N\Delta$ vertices, respectively. Again we see that the use of the exact propagator reduces the contribution drastically. This figure also shows that the consistent use of the static limit in the whole expression (i.e., static limit at the vertices together with pion range) overestimates the exact contribution by a factor of 2.

These results show that the possibility of using a reasonable value for the cutoff mass in the $N\Delta$ vertices is due to the combined use of time-ordered propagators and ρ exchange. The effect of ρ

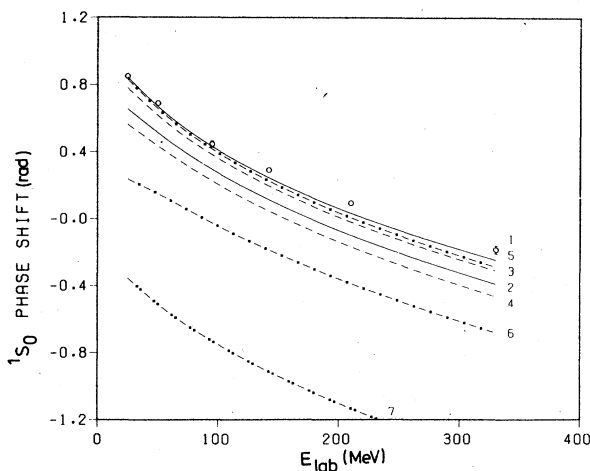


FIG. 9. Nucleon-nucleon nuclear bar phase shifts (in radians) as a function of the nucleon lab energy (in MeV). The error bars are taken from the energy-independent Livermore analysis (Ref. 19). Results for the full V_{eff} (Eq. 2.20) discussed in the text are denoted by the solid curves, with the full relativistic and static limit cases taken at all the $N\Delta$ vertices shown in curves 1 and 2, respectively. For the dashed curves, $\Delta\Delta$ contributions have been omitted from V_{eff} , in curve 3 the $\Delta\Delta$, ρ contribution is omitted, while in curve 4 the whole $\Delta\Delta$ contribution is omitted. The dashed-dot curves denote the analogous results for the $N\Delta$ contribution when the whole $\Delta\Delta$ contribution is omitted as well. For curve 5, the $\Delta\Delta$ and $N\Delta$, ρ contributions have been omitted from V_{eff} , and for curve 6, both the whole $\Delta\Delta$ and $N\Delta$ contributions have been omitted. These two curves are not shown for $T=0$ states, since $N\Delta$ states are forbidden there. The entire intermediate range attraction is left out in curve 7, i.e., the $N\Delta$, the $\Delta\Delta$ and the σ contributions have been omitted from V_{eff} .

exchange is different in various partial waves (as will be seen below by looking at the effects on the NN scattering phase shifts). In fact, ρ exchange seems to help in obtaining a consistent description of the data, see Ref. 10.

Figures 9–18 show the resulting NN scattering phase shifts, obtained by solving Eq. (2.23) numerically. The experimental error bars are taken from the energy-independent Livermore analysis.¹⁹ The solid curves show the results if the full, unapproximated V_{eff} [Eq. (2.20)] is taken, with parameters in V_{OBE} adjusted such that a reasonable description of all phase shifts is obtained. The corresponding parameters are shown in Table II. It is seen from the figures that a quantitative description of all phase shifts (like in realistic pure OBE models) is not possible at this stage (nor did we expect that). Possibly this is due to the fact that diagrams 5–12 of Fig. 1 and

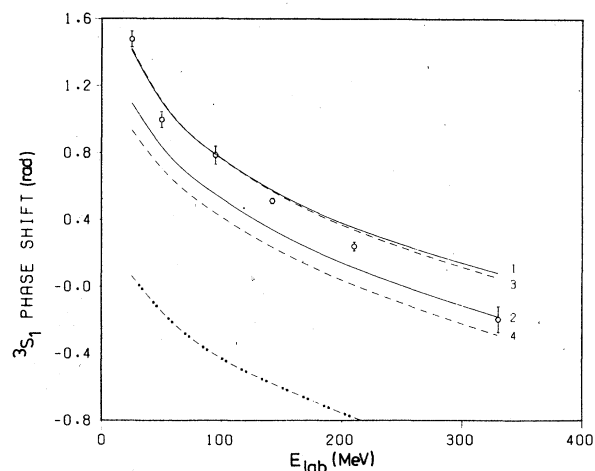


FIG. 10. (See Fig. 9.)

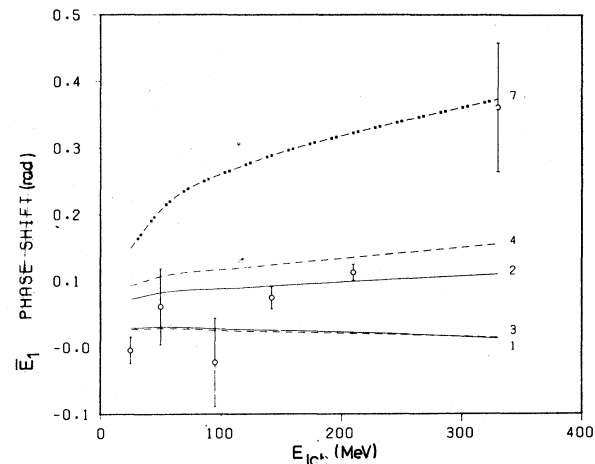


FIG. 11. (See Fig. 9.)

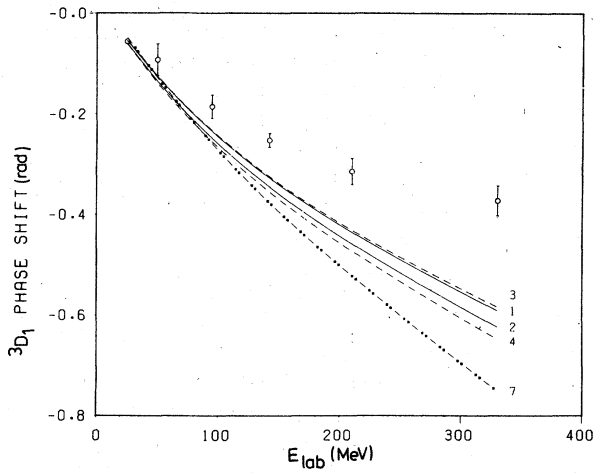


FIG. 12. (See Fig. 9.)

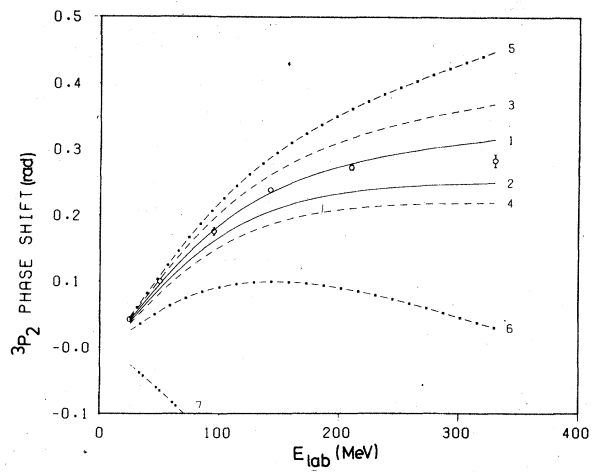


FIG. 15. (See Fig. 9.)

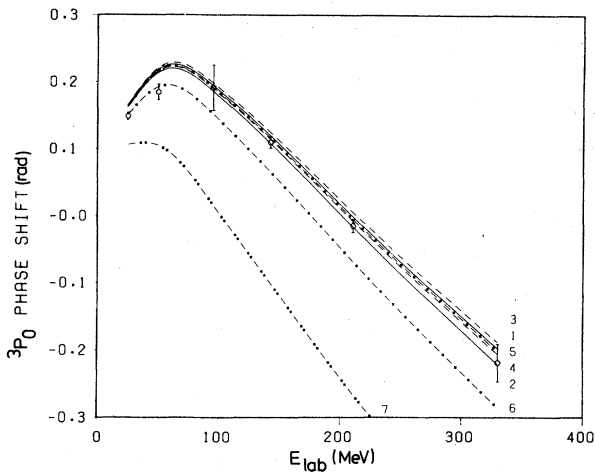


FIG. 13. (See Fig. 9.)

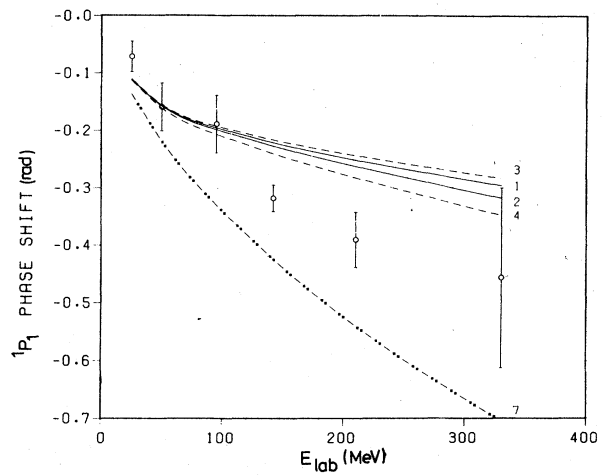


FIG. 16. (See Fig. 9.)

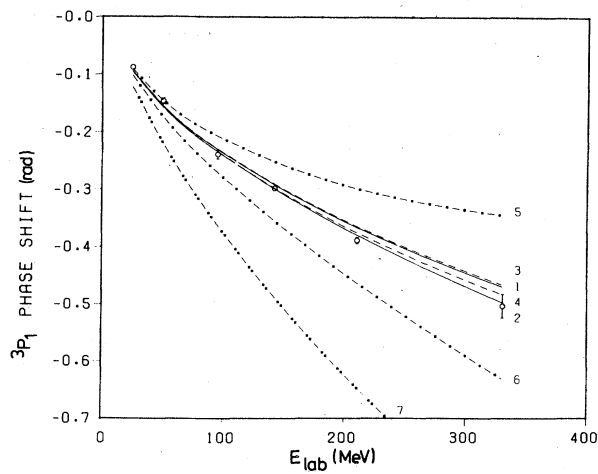


FIG. 14. (See Fig. 9.)

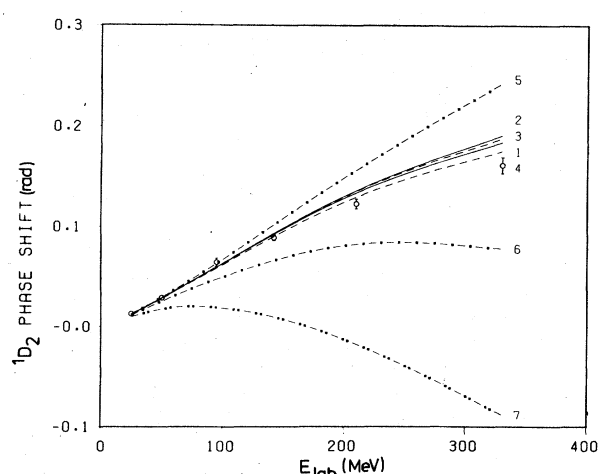


FIG. 17. (See Fig. 9.)

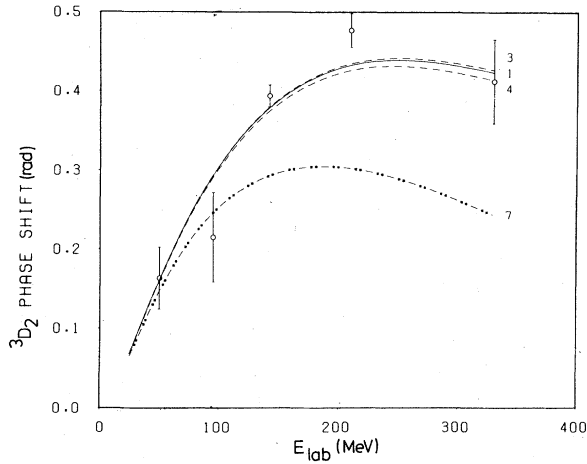


FIG. 18. The same notation as in Fig. 9–17 is used here except that curve 2 has been omitted since it cannot be distinguished from curve 1 in the figure.

the corresponding diagrams involving two-nucleon and two-isobar states have still to be included. (At the moment they are effectively described by part of the phenomenological σ meson). In other words, we are rather sure that an extension of the simple OBE model must include all diagrams of Fig. 1 (plus the noniterative diagrams involving two-nucleon intermediate states) before a quantitative description of the data can be expected again. Nevertheless, we strongly believe that one should proceed step by step and study the effects separately. The present description of the data is good enough to study specific features of the isobar contributions (i) in two-body scattering, which is the main goal here, and (ii) in nuclear structure, which is done in a separate paper.²⁰

All other curves in Figs. 9–18 are obtained by making certain approximations and by omitting specific contributions in V_{OBE} , i.e., the parameters are always kept the same. Curve 2 gives the result if the static limit is taken at all $N\Delta$ vertices. The dashed curves (curves 3 and 4) show the results if $\Delta\Delta$ contributions are omitted; in curve 3 the ρ meson in the $\Delta\Delta$ contribution is omitted, whereas for curve 4 the whole $\Delta\Delta$ contribution is

omitted. The dashed-dot curves (curves 5 and 6) show the analogous results for the $N\Delta$ contributions when the whole $\Delta\Delta$ contribution is omitted as well. The dashed-double-dot curve (curve 7) is obtained by omitting, in addition to the whole ($N\Delta + \Delta\Delta$) contribution, also the σ contribution, i.e., the total intermediate-range attraction is left out. Thus, going from curve 6 to curve 4 shows the effect of introducing the whole $N\Delta$ contribution, whereas the step from curve 4 to curve 1 gives the effect of the whole $\Delta\Delta$ contribution. Going from curve 5 to curve 4 shows the effect of the $N\Delta, \rho$ contribution separately, and the step from curve 3 to curve 1 gives the $\Delta\Delta, \rho$ contribution. Going from curve 4 to curve 3 gives the effect of the $\Delta\Delta, \pi$ contribution, whereas the step from curve 6 to curve 5 gives the $N\Delta, \pi$ contribution. There are, of course, no dashed-dot curves (curves 5 and 6) for isospin-zero states, since $N\Delta$ states are forbidden there.

The figures show that the use of the static limit at the $N\Delta$ vertices in general reduces the isobar contribution (apart from 1D). The effect is large in S waves. In 3S_1 , for example, where only $\Delta\Delta$ states contribute, the isobar contribution is reduced to roughly one third of its original value. Figure 7 showed that also in 1S_0 the main effect comes from the $\Delta\Delta$ contribution, i.e., the $N\Delta$ contribution does not change appreciably if the static limit is used, see also Ref. 10. This is plausible, since, due to its shorter range, the $\Delta\Delta$ contribution is more determined by higher-momentum components, which, in turn, are more affected by the static limit. Thus, the effects of going to the static limit cannot be neglected anymore, in contrast to Ref. 9, where the artificially strong cutoff ($\Lambda_\pi \sim 600$ MeV) suppressed strongly any effects in the high-momentum components. Furthermore, the relativistic $N\Delta$ vertex can only partially be mocked up by increasing, e.g., the σ contribution, since the effect is different in different partial waves.

The effect of the $\Delta\Delta$ contribution is comparable to the $N\Delta$ contribution in the 1S_0 partial wave, but is reduced in higher partial waves due to its comparatively shorter range, especially the $\Delta\Delta, \rho$

TABLE II. Parameters for V_{OBE} defined in the text. Here m_α and Λ_α are given in MeV. The number in brackets denotes the ratio of coupling constants f_ρ/g_ρ .

	π	η	σ	δ	ω	ρ	ϕ
g_α^2	14.4	4.9978	13.5416	0.0718	30.012	0.4701 (6.61)	5.3613
m_α	138	548.5	599.7	960	782.8	712	1020
Λ_α	2000	2000	1300	1300	1650	1650	1650

TABLE III. Low-energy scattering and deuteron data. Here E , Q , and P_D are the binding energy, quadrupole moment and D -state probability of the deuteron, respectively. Also, a_s and a_t are the singlet and triplet scattering lengths while r_s and r_t are the singlet and triplet effective ranges, respectively.

	Exp.	Theory
E (MeV)	2.22462 ± 0.00006	2.2249
Q (fm ²)	0.2860 ± 0.0015	0.280
P_D (%)	5 \pm 2	4.50
a_s (fm)	-23.715 ± 0.015	-23.70
r_s (fm)	2.73 \pm 0.03	2.74
a_t (fm)	5.423 ± 0.005	5.40
r_t (fm)	1.748 \pm 0.014	1.72

contribution is strongly suppressed in waves ($L \geq 1$). In general, ρ exchange acts opposite to π exchange; the role of ρ exchange is nicely demonstrated, e.g., in the 3P_1 partial wave. In fact, the inclusion of ρ exchange helps in obtaining a consistent description of the important 3P states, see also Ref. 10. Note that our total Δ contribution has roughly the same strength as the version in Ref. 9 with $\Lambda_r \sim 700$ MeV. With such a cutoff mass, typical discrepancies showed up in Ref. 9 for 3P states and 1D_2 . The present figures show that ρ exchange partly removes these discrepancies.

Compared to the former procedure in Ref. 9 (where the simple pion-range propagator was used), the total Δ contribution is now suppressed much more in higher partial waves. This feature can be traced back to the much shorter range generated by the retardation effects of the time-ordered propagators.

Finally, the low-energy scattering and deuteron data determined from the exact V_{eff} are given in Table III. Note the small value of the D state probability in spite of the relatively weak πNN form factor used here. This feature can be traced back to the retardation effects of the time-ordered propagators, which suppress higher-order contributions in V_{eff} , i.e., contributions coming from the tensor force. Thus, it is possible to obtain a low D state probability (which nowadays seems to be favored by certain few-body reactions²¹) without using an unreasonably strong πNN form factor.

IV. CONCLUDING REMARKS

In this paper, we have calculated the fourth-order iterative diagrams involving $N\Delta$ and $\Delta\Delta$ intermediate states and including π as well as ρ exchange in the framework of "old fashioned" perturbation theory. The neglect of retardation ef-

fects in the time-ordered propagators (which results in the simple propagators of pion, respectively, ρ range) leads to a serious overestimate of the isobar contributions by as much as a factor of 3. On the other hand, the static limit underestimates the contribution by roughly a factor of 2. Therefore, the combined use of (a) pion-range and ρ -range propagators in the transition potential and (b) the static limit (which is necessarily performed by groups working in r space) overestimates the isobar contribution by roughly a factor of 2. This is in line with the dispersion-theoretical results of Ref. 15 based on empirical amplitudes for $NN \rightarrow 2\pi$ in the pseudophysical region. However, since this factor is slightly different in different partial waves, the approximations (a) and (b) cannot adequately be mocked up by a mere change of parameters.

NN scattering phase shifts have been calculated using these diagrams together with a suitably modified OBE potential. It turned out that the effect of the $N\Delta\rho$ vertex is different in different partial waves; this feature helps to improve the description especially of the important 3P partial wave phase shifts. The overall agreement with empirical data is good enough to allow a meaningful calculation of binding energies of nuclei. The results of such calculations are reported in a separate paper.²⁰ On the other hand, the slight, but characteristic discrepancies between theoretical and empirical phase shifts in some partial waves suggest an extension of the present model. The next step is to also include the noniterative diagrams of Fig. 1 together with those involving intermediate NN and $\Delta\Delta$ states. This problem is presently being attacked by the present authors and will be the subject of a forthcoming paper.

Many stimulating discussions with Professor K. Bleuler are gratefully acknowledged.

APPENDIX

Here we give the results for some matrix elements of our ρ exchange transition potentials, which are needed in order to describe NN scattering. Here \vec{q} is parallel to the z axis, \vec{q}' lies in the xz plane and ϑ is the angle between \vec{q} and \vec{q}' . We first define the following quantities:

$$A_{\pm} = \left(1 \pm \frac{q'q}{W'W}\right), \quad A_{\pm}^* = \left(1 \pm \frac{q'q}{W'W^*}\right),$$

$$B_{\pm} = \left(\frac{q'}{W'} \pm \frac{q}{W}\right), \quad B_{\pm}^* = \left(\frac{q'}{W'} \pm \frac{q}{W^*}\right),$$

where $W = E_q + M$, $W' = E_{q'} + M$, and $W^* = E_q^* + M_{\Delta}$. Furthermore,

$$D_{N\Delta} = \frac{4\pi}{(2\pi)^3} \frac{f_{N\Delta\rho}}{m_\rho} \frac{W'}{4E_q} \left(\frac{W^*W}{E_q^*E_q} \right)^{1/2} \\ \times \frac{C_{N\Delta}(I)F_\rho}{2\omega_\rho(E_q' + E_q + \omega_\rho - z)},$$

$$D_{\Delta\Delta} = -\frac{4\pi}{(2\pi)^3} \frac{f_{N\Delta\rho}}{m_\rho^2} \frac{W'W^*}{4E_qE_q^*} \frac{C_{\Delta\Delta}(I)F_\rho}{2\omega_\rho(E_q' + E_q^* + \omega_\rho - z)},$$

where $C_{N\Delta}(I)$, $C_{\Delta\Delta}(I)$ are appropriate isospin factors, I being the isospin of the two-baryon system:

$$C_{N\Delta}(0) = 0, \quad C_{N\Delta}(1) = \left(\frac{2}{3}\right)^{1/2};$$

$$C_{\Delta\Delta}(0) = -\sqrt{2}, \quad C_{\Delta\Delta}(1) = -\left(\frac{10}{9}\right)^{1/2}$$

We start with $V_{N\Delta,1}^\rho$, i.e., Eq. (2.13):

$$\langle \bar{q}'_{\frac{1}{2}\frac{1}{2}} | V_{N\Delta,1}^\rho | \bar{q}_{\frac{1}{2}\frac{3}{2}} \rangle = D_{N\Delta} \left(\frac{1}{2}\right)^{1/2} \sin\vartheta \left[\left((g_\rho + f_\rho) \left[\frac{1}{2}q'A_+B_+^* + \left(\frac{1}{2}q' + q\right)A_+^*B_+ \right] \right. \right. \\ \left. \left. - \frac{f_\rho}{2M} \left[\frac{1}{2}q'(E_q' + E_q)A_-B_+^* + q'A_-A_+^* - \left(\frac{1}{2}q' + q\right)(E_q' - E_q)A_+^*B_- \right] \right. \right. \\ \left. \left. + \frac{1}{2}q' \left((g_\rho + f_\rho)(A_+B_+^* - A_+^*B_+) - \frac{f_\rho}{2M} \left[(E_q' + E_q)A_-B_+^* \right. \right. \right. \right. \\ \left. \left. \left. + 2qA_-A_+^* + (E_q' - E_q)A_+^*B_- \right] \right) \cos\vartheta \right],$$

$$\langle \bar{q}'_{\frac{1}{2}\frac{1}{2}} | V_{N\Delta,1}^\rho | \bar{q}_{\frac{1}{2}\frac{1}{2}} \rangle = D_{N\Delta} \left(\frac{1}{2}\right)^{1/2} q' \sin^2\vartheta \left((g_\rho + f_\rho)(A_+B_+^* - A_+^*B_+) - \frac{f_\rho}{2M} \left[(E_q' + E_q)A_-B_+^* - 2qA_-A_+^* + (E_q' - E_q)A_+^*B_- \right] \right),$$

$$\langle \bar{q}'_{\frac{1}{2}\frac{1}{2}} | V_{N\Delta,1}^\rho | \bar{q}_{\frac{1}{2}\frac{1}{2}} \rangle = D_{N\Delta} \left(\frac{1}{6}\right)^{1/2} \left\{ (g_\rho + f_\rho) \left(\left(\frac{1}{2}q' - q\right)A_+B_+^* - \left(\frac{1}{2}q' + q\right)A_+^*B_+ - 2\frac{q}{M_\Delta} (q' + q)B_+^*B_+ - \frac{E_q^*}{M_\Delta} q'(A_+B_+^* - A_+^*B_+) \right. \right. \\ \left. \left. - \frac{f_\rho}{2M} \left[(E_q' + E_q) \left(\frac{1}{2}q' - q\right)A_-B_+^* - q'A_-A_+^* - \left[(E_q' + E_q)E_q^* + 2q^2 \right] \frac{q'}{M_\Delta} A_-B_+^* \right. \right. \right. \\ \left. \left. \left. + (E_q' - E_q) \left(\left(\frac{1}{2}q' + q\right)A_+^*B_- + 2\frac{q}{M_\Delta} (q' + q)B_+^*B_- - \frac{E_q^*}{M_\Delta} q'A_+^*B_- \right) \right] \right\} \\ + \left[(g_\rho + f_\rho) \left((q' - q)A_+B_+^* + (q' + q)A_+^*B_+ + 2\frac{q}{M_\Delta} (q' + q)B_+^*B_+ \right) \right. \\ \left. - \frac{f_\rho}{2M} \left((E_q' + E_q)(q' - q)A_-B_+^* - (E_q' - E_q)(q' + q)A_+^*B_- \right. \right. \\ \left. \left. - 2(E_q' - E_q) \frac{q}{M_\Delta} (q' + q)B_+^*B_- \right) \right] \cos\vartheta \\ + q' \left[(g_\rho + f_\rho) \left(\frac{1}{2}(A_+B_+^* - A_+^*B_+) + \frac{E_q^*}{M_\Delta} (A_+B_+^* - A_+^*B_+) \right) - \frac{f_\rho}{2M} (qA_-A_+^* + \frac{1}{2}(E_q' + E_q)A_-B_+^* \right. \right. \\ \left. \left. + \left(\frac{E_q^*}{M_\Delta} (E_q' + E_q) + 2\frac{q^2}{M_\Delta} \right) A_-B_+^* + (E_q' - E_q) \left(\frac{1}{2}A_+^*B_- + \frac{E_q^*}{M_\Delta} A_+^*B_- \right) \right] \cos^2\vartheta \right\},$$

$$\langle \bar{q}'_{\frac{1}{2}\frac{1}{2}} | V_{N\Delta,1}^\rho | \bar{q}_{\frac{1}{2}\frac{1}{2}} \rangle = D_{N\Delta} \left(\frac{1}{6}\right)^{1/2} \sin\vartheta \left\{ (g_\rho + f_\rho) \left(\left(\frac{1}{2}q' + q\right)A_+B_+^* + \frac{1}{2}q'A_+^*B_+ - \frac{q'}{M_\Delta} \left[E_q^*(A_+B_+^* + A_+^*B_+) + 2qB_+^*B_+ \right] \right. \right. \\ \left. \left. - \frac{f_\rho}{2M} \left[(E_q' + E_q) \left(\frac{1}{2}q' + q\right)A_-B_+^* + q'A_-A_+^* - \frac{q'}{M_\Delta} \left[(E_q' + E_q)E_q^* + 2q^2 \right] A_-B_+^* \right. \right. \right. \\ \left. \left. \left. - (E_q' - E_q) \left(\frac{1}{2}q'A_+^*B_- - \frac{q'}{M_\Delta} E_q^*A_+^*B_- - 2q \frac{q'}{M_\Delta} B_+^*B_- \right) \right] \right\} \\ + q' \left\{ (g_\rho + f_\rho) \left(\frac{1}{2}(A_+^*B_+ - A_+B_+^*) - \frac{E_q^*}{M_\Delta} (A_+B_+^* - A_+^*B_+) \right) \right. \\ \left. + \frac{f_\rho}{2M} \left[\frac{1}{2}(E_q' + E_q)A_-B_+^* - qA_+^*A_- + \left((E_q' + E_q) \frac{E_q^*}{M_\Delta} + 2\frac{q^2}{M_\Delta} \right) A_-B_+^* \right. \right. \\ \left. \left. + (E_q' - E_q) \left(\frac{1}{2}A_+^*B_- + \frac{E_q^*}{M_\Delta} A_+^*B_- \right) \right] \right\} \cos\vartheta \right\},$$

$$\begin{aligned}
\langle \tilde{q}'_{\frac{1}{2}} - \frac{1}{2} | V_{N\Delta,1}^{\rho} | \tilde{q}_{\frac{1}{2}} - \frac{3}{2} \rangle &= D_{N\Delta} \frac{1}{2} (\frac{1}{2})^{1/2} q' \sin\vartheta (1 + \cos\vartheta) \left((g_{\rho} + f_{\rho})(A_{+}B_{+}^{*} + A_{+}^{*}B_{+}) \right. \\
&\quad \left. - \frac{f_{\rho}}{2M} [(E_{q'} + E_q)A_{-}B_{+}^{*} + 2qA_{-}A_{+}^{*} - (E_{q'} - E_q)A_{+}^{*}B_{-}] \right), \\
\langle \tilde{q}'_{\frac{1}{2}} - \frac{1}{2} | V_{N\Delta,1}^{\rho} | \tilde{q}_{\frac{3}{2}} \rangle &= -D_{N\Delta} (\frac{1}{2})^{1/2} (1 - \cos\vartheta) \left[\left((g_{\rho} + f_{\rho})[\frac{1}{2}q'A_{+}B_{+}^{*} - (\frac{1}{2}q' + q)A_{+}^{*}B_{+}] \right. \right. \\
&\quad \left. \left. + \frac{f_{\rho}}{2M} [q'qA_{-}A_{+}^{*} - \frac{1}{2}q'(E_{q'} + E_q)A_{-}B_{+}^{*} - (\frac{1}{2}q' + q)(E_{q'} - E_q)A_{+}^{*}B_{-}] \right) \right. \\
&\quad \left. + \frac{1}{2}q' \left((g_{\rho} + f_{\rho})(A_{+}B_{+}^{*} + A_{+}^{*}B_{+}) \right. \right. \\
&\quad \left. \left. + \frac{f_{\rho}}{2M} [2qA_{-}A_{+}^{*} - (E_{q'} + E_q)A_{-}B_{+}^{*} + (E_{q'} - E_q)A_{+}^{*}B_{-}] \right) \cos\vartheta \right], \\
\langle \tilde{q}'_{\frac{1}{2}} - \frac{1}{2} | V_{N\Delta,1}^{\rho} | \tilde{q}_{\frac{3}{2}} \rangle &= D_{N\Delta} (\frac{1}{8})^{1/2} \sin\vartheta \left\{ (g_{\rho} + f_{\rho}) \left((\frac{1}{2}q' + q)(A_{+}B_{+}^{*} + A_{+}^{*}B_{+}) - \frac{E_q^{*}}{M_{\Delta}} q'(A_{+}B_{+}^{*} - A_{+}^{*}B_{+}) - 2\frac{q^2}{M_{\Delta}} B_{+}B_{+}^{*} \right) \right. \\
&\quad \left. - \frac{f_{\rho}}{2M} [(E_{q'} + E_q)(\frac{1}{2}q' + q)A_{-}B_{+}^{*} + q'qA_{+}^{*}A_{-} - \frac{q'}{M_{\Delta}} [(E_{q'} + E_q)E_q^{*} + 2q^2]A_{-}B_{+}^{*} \right. \\
&\quad \left. - (E_{q'} - E_q) \left((\frac{1}{2}q' + q)A_{+}^{*}B_{-} + \frac{E_q^{*}}{M_{\Delta}} q'A_{+}^{*}B_{-} - 2\frac{q^2}{M_{\Delta}} B_{+}^{*}B_{-} \right) \right\} \\
&\quad - q' \left\{ (g_{\rho} + f_{\rho}) \left(\frac{1}{2}(A_{+}B_{+}^{*} + A_{+}^{*}B_{+}) + \frac{E_q^{*}}{M_{\Delta}} (A_{+}B_{+}^{*} + A_{+}^{*}B_{+}) \right) \right. \\
&\quad \left. + \frac{f_{\rho}}{2M} \left[qA_{+}^{*}A_{-} - \frac{1}{2}(E_{q'} + E_q)A_{-}B_{+}^{*} - \frac{1}{M_{\Delta}} [(E_{q'} + E_q) + 2q^2]A_{-}B_{+}^{*} \right. \right. \\
&\quad \left. \left. + (E_{q'} - E_q) \left(\frac{1}{2}A_{+}^{*}B_{-} + \frac{E_q^{*}}{M_{\Delta}} A_{+}^{*}B_{-} \right) \right] \right\} \cos\vartheta, \\
\langle \tilde{q}'_{\frac{1}{2}} - \frac{1}{2} | V_{N\Delta,1}^{\rho} | \tilde{q}_{\frac{1}{2}} - \frac{1}{2} \rangle &= D_{N\Delta} (\frac{1}{8})^{1/2} (1 + \cos\vartheta) \left\{ (g_{\rho} + f_{\rho}) \left(\frac{1}{2}q'A_{+}^{*}B_{+} - (\frac{1}{2}q' - q)A_{+}B_{+}^{*} + \frac{E_q^{*}}{M_{\Delta}} q'(A_{+}B_{+}^{*} + A_{+}^{*}B_{+}) \right) \right. \\
&\quad \left. - \frac{f_{\rho}}{2M} \left[q'qA_{-}A_{+}^{*} - (\frac{1}{2}q' - q)(E_{q'} + E_q)A_{-}B_{+}^{*} \right. \right. \\
&\quad \left. \left. + \frac{q'}{M_{\Delta}} [(E_{q'} + E_q)E_q^{*} + 2q^2]A_{-}B_{+}^{*} \right. \right. \\
&\quad \left. \left. - (E_{q'} - E_q) \frac{1}{2}q' \left(A_{+}^{*}B_{-} + 2\frac{E_q^{*}}{M_{\Delta}} A_{+}^{*}B_{-} \right) \right] \right\} \\
&\quad - q' \left\{ (g_{\rho} + f_{\rho}) \left(\frac{1}{2}(A_{+}B_{+}^{*} + A_{+}^{*}B_{+}) + \frac{E_q^{*}}{M_{\Delta}} (A_{+}B_{+}^{*} + A_{+}^{*}B_{+}) \right) \right. \\
&\quad \left. - \frac{f_{\rho}}{2M} \left[\frac{1}{2}(E_{q'} + E_q)A_{-}B_{+}^{*} + qA_{-}A_{+}^{*} + \frac{1}{M_{\Delta}} [(E_{q'} + E_q)E_q^{*} + 2q^2]A_{-}B_{+}^{*} \right. \right. \\
&\quad \left. \left. - (E_{q'} - E_q) \left(\frac{1}{2}A_{+}^{*}B_{-} + \frac{E_q^{*}}{M_{\Delta}} A_{+}^{*}B_{-} \right) \right] \right\} \cos\vartheta.
\end{aligned}$$

Also $\langle \tilde{q}'_{\frac{1}{2}} | V_{N\Delta,1}^{\rho} | \tilde{q} - \Lambda_1 - \Lambda_2 \rangle$ can be obtained from $\langle \tilde{q}'_{\frac{1}{2}} | V_{N\Delta,1}^{\rho} | \tilde{q} \Lambda_1 \Lambda_2 \rangle$ by replacing there $(q, \cos\vartheta)$ by $(-q, -\cos\vartheta)$ and $\langle \tilde{q}'_{\frac{1}{2}} - \frac{1}{2} | V_{N\Delta,1}^{\rho} | \tilde{q} - \Lambda_1 - \Lambda_2 \rangle$ can be obtained from $-\langle \tilde{q}'_{\frac{1}{2}} - \frac{1}{2} | V_{N\Delta,1}^{\rho} | \tilde{q} \Lambda_1 \Lambda_2 \rangle$ by the same replacement. We now present the results for $V_{\Delta\Delta,1}^{\rho}$, i.e., Eq. (2.16):

$$\langle \tilde{q}'_{\frac{1}{2}} | V_{\Delta\Delta,1}^{\rho} | \tilde{q}_{\frac{3}{2}} \rangle = D_{\Delta\Delta} \frac{1}{4} (1 + \cos\vartheta) \{ [(q'^2 + 2q^2)A_{+}^{*2} + q'^2 B_{+}^{*2}] - 4q'qA_{+}^{*2} \cos\vartheta + q'^2(A_{+}^{*2} - B_{+}^{*2}) \cos\vartheta \},$$

$$\langle \tilde{q}'_{\frac{1}{2}} | V_{\Delta\Delta,1}^{\rho} | \tilde{q}_{\frac{3}{2}} - \frac{3}{2} \rangle = -D_{\Delta\Delta} \frac{1}{4} q'^2 (A_{+}^{*}A_{+}^{*} - B_{+}^{*}B_{+}^{*}) \sin^3\vartheta,$$

$$\langle \vec{q}'_{\frac{1}{2}\frac{1}{2}} | V_{\Delta\Delta,1}^{\rho} | \vec{q}_{\frac{3}{2}\frac{1}{2}} - \frac{1}{2} \rangle = D_{\Delta\Delta} \sin^2 \vartheta \frac{1}{4} \left(\frac{1}{3} \right)^{1/2} q' \left[\left(q' A_{+}^{*2} + (q' + 2q) B_{+}^{*2} - 2 \frac{E_q^*}{M_{\Delta}} (q A_{+}^* A_{-}^* + q' B_{+}^* B_{-}^*) - 2 \frac{q}{M_{\Delta}} (q' + q) A_{+}^* B_{-}^* \right) \right. \\ \left. + q' \left(A_{+}^{*2} - B_{+}^{*2} + 2 \frac{E_q^*}{M_{\Delta}} (A_{+}^* A_{-}^* - B_{+}^* B_{-}^*) \right) \cos \vartheta \right],$$

$$\langle \vec{q}'_{\frac{1}{2}\frac{1}{2}} | V_{\Delta\Delta,1}^{\rho} | \vec{q}_{\frac{3}{2}\frac{1}{2}} \rangle = -D_{\Delta\Delta} \frac{1}{2} \left(\frac{1}{3} \right)^{1/2} \sin \vartheta \left[\left(\left(\frac{1}{2} q'^2 + q^2 \right) A_{+}^* A_{-}^* - \frac{E_q^*}{M_{\Delta}} q' q A_{+}^{*2} + \frac{q}{M_{\Delta}} (q'^2 + q'q + 2q^2) A_{+}^* B_{-}^* \right. \right. \\ \left. \left. - \frac{1}{2} q' (q' - 2q) B_{+}^* B_{-}^* + \frac{E_q^*}{M_{\Delta}} q'^2 B_{+}^{*2} \right) \right. \\ \left. - q' \left(2q A_{+}^* A_{-}^* - \frac{E_q^*}{M_{\Delta}} (q' - q) A_{+}^{*2} + \frac{q}{M_{\Delta}} (q' + 3q) A_{+}^* B_{-}^* + (q' - q) B_{+}^* B_{-}^* \right) \cos \vartheta \right. \\ \left. + q'^2 \left(\frac{1}{2} (A_{+}^* A_{-}^* - B_{+}^* B_{-}^*) + \frac{E_q^*}{M_{\Delta}} (A_{+}^{*2} - B_{+}^{*2}) \right) \cos^2 \vartheta \right],$$

$$\langle \vec{q}'_{\frac{1}{2}\frac{1}{2}} | V_{\Delta\Delta,1}^{\rho} | \vec{q}_{\frac{1}{2}\frac{1}{2}} \rangle = -D_{\Delta\Delta} \frac{1}{6} \left[\left(-2q' q \frac{E_q^*}{M_{\Delta}} A_{+}^* A_{-}^* + \left(\frac{1}{2} q'^2 + q^2 \right) A_{-}^{*2} + 2 \frac{E_q^{*2}}{M_{\Delta}^2} q'^2 A_{+}^{*2} - 4 \frac{q E_q^*}{M_{\Delta}^2} q' (q' + q) A_{+}^* B_{-}^* \right. \right. \\ \left. \left. + 2 \frac{q}{M_{\Delta}} (q'^2 + q'q + 2q^2) A_{+}^* B_{-}^* - 2 \frac{E_q^*}{M_{\Delta}} q' (q' - 2q) B_{+}^* B_{-}^* \right. \right. \\ \left. \left. + \left(\frac{1}{2} q'^2 - 2q'q + 2q^2 \right) B_{-}^{*2} + \frac{4}{M_{\Delta}^2} \left[\frac{1}{2} q'^2 E_q^{*2} + q^2 (q'^2 + q'q + q^2) \right] B_{+}^{*2} \right) \right. \\ \left. + \left(2q'^2 \frac{E_q^*}{M_{\Delta}} A_{+}^* A_{-}^* - \left(\frac{1}{2} q'^2 + 2q'q + q^2 \right) A_{-}^{*2} + 2q'^2 \frac{E_q^{*2}}{M_{\Delta}^2} A_{+}^{*2} - 4 \frac{q}{M_{\Delta}} (q' + q)^2 A_{+}^* B_{-}^* \right. \right. \\ \left. \left. - 2q'^2 \frac{E_q^*}{M_{\Delta}} B_{+}^* B_{-}^* + \left(\frac{3}{2} q'^2 - 4q'q + 2q^2 \right) B_{-}^{*2} - \frac{4}{M_{\Delta}^2} \left(\frac{1}{2} q'^2 E_q^{*2} + q^2 (q' + q)^2 \right) B_{+}^{*2} \right) \cos \vartheta \right. \\ \left. + q' \left(2q \frac{E_q^*}{M_{\Delta}} A_{+}^* A_{-}^* + \left(\frac{1}{2} q' + 2q \right) A_{-}^{*2} - 2q' \frac{E_q^{*2}}{M_{\Delta}^2} A_{+}^{*2} \right. \right. \\ \left. \left. + 4(q' + q) \frac{q E_q^*}{M_{\Delta}^2} A_{+}^* B_{-}^* + 2 \frac{q}{M_{\Delta}} (q' + 3q) A_{+}^* B_{-}^* \right. \right. \\ \left. \left. + 2(q' - 2q) \frac{E_q^*}{M_{\Delta}} B_{+}^* B_{-}^* + \left(\frac{3}{2} q' - 2q \right) B_{-}^{*2} - \frac{2}{M_{\Delta}^2} (q' E_q^{*2} - 2q^3) B_{+}^{*2} \right) \cos^2 \vartheta \right. \\ \left. - q'^2 \left[\frac{1}{2} (A_{-}^{*2} B_{-}^{*2}) + 2 \frac{E_q^{*2}}{M_{\Delta}^2} (A_{+}^{*2} - B_{+}^{*2}) + 2 \frac{E_q^*}{M_{\Delta}} (A_{+}^* A_{-}^* - B_{+}^* B_{-}^*) \right] \cos^3 \vartheta \right],$$

$$\langle \vec{q}'_{\frac{1}{2}\frac{1}{2}} | V_{\Delta\Delta,1}^{\rho} | \vec{q}_{\frac{1}{2}\frac{1}{2}} - \frac{1}{2} \rangle = -D_{\Delta\Delta} \frac{1}{6} \sin \vartheta \left\{ \left[\frac{1}{2} q'^2 \left(1 + 4 \frac{E_q^{*2}}{M_{\Delta}^2} \right) A_{+}^* A_{-}^* - q' q \frac{E_q^*}{M_{\Delta}} (A_{+}^{*2} - A_{-}^{*2}) \right. \right. \\ \left. \left. - q' (q' - q) \frac{q}{M_{\Delta}} A_{+}^* B_{-}^* - 2q' (q' - q) \frac{q E_q^*}{M_{\Delta}^2} A_{+}^* B_{-}^* - q' (q' - 2q) \frac{E_q^*}{M_{\Delta}} B_{-}^{*2} \right. \right. \\ \left. \left. + 2q' (q' + q) \frac{q E_q^*}{M_{\Delta}^2} A_{+}^* B_{-}^* + q' (q' + q) \frac{q}{M_{\Delta}} A_{+}^* B_{-}^* - q' (q' + 2q) \frac{E_q^*}{M_{\Delta}} B_{+}^{*2} \right. \right. \\ \left. \left. + \left(2 \frac{q'^2}{M_{\Delta}^2} (E_q^{*2} + 2q^2) + \frac{q'^2}{2} - 2q^2 \right) B_{+}^* B_{-}^* \right] \right. \\ \left. + q' \left[\frac{E_q^*}{M_{\Delta}} (q' - q) A_{+}^{*2} - \frac{E_q^*}{M_{\Delta}} (q' + q) A_{-}^{*2} - (q' - q) \frac{q}{M_{\Delta}} A_{+}^* B_{-}^* - 2(q' - q) \frac{q E_q^*}{M_{\Delta}^2} A_{+}^* B_{-}^* \right. \right. \\ \left. \left. - (q' + q) \frac{q}{M_{\Delta}} A_{+}^* B_{-}^* + 2q \left(1 - 2 \frac{q^2}{M_{\Delta}^2} \right) B_{+}^* B_{-}^* - 2(q' + q) \frac{q E_q^*}{M_{\Delta}^2} A_{+}^* B_{-}^* \right. \right. \\ \left. \left. + 2(q' + q) \frac{E_q^*}{M_{\Delta}} B_{+}^{*2} - 2(q' - q) \frac{E_q^*}{M_{\Delta}} B_{-}^{*2} \right] \cos \vartheta \right. \\ \left. + q'^2 \left[\left(\frac{1}{2} + 2 \frac{E_q^{*2}}{M_{\Delta}^2} \right) (A_{+}^* A_{-}^* - B_{+}^* B_{-}^*) + \frac{E_q^*}{M_{\Delta}} (A_{-}^{*2} - B_{-}^{*2} + A_{+}^{*2} - B_{+}^{*2}) \right] \cos^2 \vartheta \right\},$$

$$\langle \bar{q}'_{\frac{1}{2}} - \frac{1}{2} | V_{\Delta\Delta,1}^0 | \bar{q}_{\frac{3}{2}}^{\frac{3}{2}} \rangle = -D_{\Delta\Delta\frac{1}{4}} \sin\vartheta \{ [-(q'^2 + 2q^2)A_+^*A_-^* + q'^2 B_+^*B_-^*] + 4q'qA_+^*A_-^* \cos\vartheta - q'^2(A_+^*A_-^* + B_+^*B_-^*) \cos^2\vartheta \},$$

$$\langle \bar{q}'_{\frac{1}{2}} - \frac{1}{2} | V_{\Delta\Delta,1}^0 | \bar{q}_{\frac{3}{2}}^{\frac{3}{2}} - \frac{3}{2} \rangle = D_{\Delta\Delta\frac{1}{4}} q'^2 \sin^2\vartheta (1 + \cos\vartheta) (A_+^{*2} + B_+^{*2}),$$

$$\langle \bar{q}'_{\frac{1}{2}} - \frac{1}{2} | V_{\Delta\Delta,1}^0 | \bar{q}_{\frac{3}{2}}^{\frac{3}{2}} - \frac{1}{2} \rangle = D_{\Delta\Delta\frac{1}{4}} (\frac{1}{3})^{1/2} q' \sin\vartheta (1 + \cos\vartheta) \left[\left(q'A_+^*A_-^* + 2q \frac{E_q^*}{M_\Delta} A_+^{*2} + 2 \frac{q}{M_\Delta} (q' - q) A_+^*B_+^* \right. \right. \\ \left. \left. - (q' - 2q) B_+^*B_-^* + 2q' \frac{E_q^*}{M_\Delta} B_+^{*2} \right) \right. \\ \left. - q' \left(A_+^*A_-^* + B_+^*B_-^* + 2 \frac{E_q^*}{M_\Delta} (A_+^{*2} + B_+^{*2}) \right) \cos\vartheta \right],$$

$$\langle \bar{q}'_{\frac{1}{2}} - \frac{1}{2} | V_{\Delta\Delta,1}^0 | \bar{q}_{\frac{3}{2}}^{\frac{3}{2}} \frac{1}{2} \rangle = D_{\Delta\Delta\frac{1}{2}} (\frac{1}{3})^{1/2} (1 + \cos\vartheta) \left[\left(\frac{E_q^*}{M_\Delta} q'qA_+^*A_-^* + (\frac{1}{2}q'^2 + q^2)A_+^{*2} - (q'^2 - q'q + 2q^2) \frac{q}{M_\Delta} A_+^*B_+^* \right. \right. \\ \left. \left. - \frac{E_q^*}{M_\Delta} q'^2 B_+^*B_-^* + q'(\frac{1}{2}q'^2 + q)B_+^{*2} \right) \right. \\ \left. - q' \left(\frac{E_q^*}{M_\Delta} (q' + q)A_+^*A_-^* + 2qA_+^{*2} + (q' - 3q) \frac{q}{M_\Delta} A_+^*B_+^* + (q' - q)B_+^{*2} \right) \cos\vartheta \right. \\ \left. + q'^2 \left(\frac{1}{2}(A_+^{*2} + B_+^{*2}) + \frac{E_q^*}{M_\Delta} (A_+^*A_-^* + B_+^*B_-^*) \right) \cos^2\vartheta \right],$$

$$\langle \bar{q}'_{\frac{1}{2}} - \frac{1}{2} | V_{\Delta\Delta,1}^0 | \bar{q}_{\frac{3}{2}}^{\frac{3}{2}} \frac{1}{2} \rangle = -D_{\Delta\Delta\frac{1}{6}} \sin\vartheta \left\{ \left[\left(\frac{3}{2}q'^2 - q^2 + 2q'^2 \frac{q^2}{M_\Delta^2} \right) A_+^*A_-^* + \frac{E_q^*}{M_\Delta} q'q(A_+^{*2} - A_-^{*2}) - \frac{q}{M_\Delta} (q'^2 + q'q + 2q^2) A_+^*B_+^* \right. \right. \\ \left. \left. + 2q'(q' - q) \frac{qE_q^*}{M_\Delta^2} A_+^*B_-^* - 2q'(q' + q) \frac{qE_q^*}{M_\Delta^2} A_-^*B_+^* \right. \right. \\ \left. \left. + (q'^2 - q'q + 2q^2) \frac{q}{M_\Delta} A_-^*B_-^* - \frac{E_q^*}{M_\Delta} q'(q' + 2q)B_+^{*2} \right. \right. \\ \left. \left. + \left(\frac{5}{2}q'^2 - 2q^2 + 2q'^2 \frac{q^2}{M_\Delta^2} + 4 \frac{q^4}{M_\Delta^2} \right) B_+^*B_-^* - \frac{E_q^*}{M_\Delta} q'(q' - 2q)B_-^{*2} \right] \right. \\ \left. + q' \left[2qA_+^*A_-^* - (q' - q) \frac{E_q^*}{M_\Delta} A_+^{*2} + (q' + q) \frac{E_q^*}{M_\Delta} A_-^{*2} + (q' + 3q) \frac{q}{M_\Delta} A_+^*B_+^* \right. \right. \\ \left. \left. + 2(q' - q) \frac{qE_q^*}{M_\Delta^2} A_+^*B_-^* + 2(q' + q) \frac{qE_q^*}{M_\Delta^2} A_-^*B_+^* \right. \right. \\ \left. \left. + (q' - 3q) \frac{q}{M_\Delta} A_-^*B_-^* + 2q \left(1 - 2 \frac{q^2}{M_\Delta^2} \right) B_+^*B_-^* \right. \right. \\ \left. \left. + 2(q' + q) \frac{E_q^*}{M_\Delta} B_+^{*2} - 2(q' - q) \frac{E_q^*}{M_\Delta} B_-^{*2} \right] \cos\vartheta \right. \\ \left. + q'^2 \left[\left(\frac{1}{2} + 2 \frac{E_q^*}{M_\Delta^2} \right) (A_+^*A_-^* + B_+^*B_-^*) + \frac{E_q^*}{M_\Delta} (A_-^{*2} + B_-^{*2} + A_+^{*2} + B_+^{*2}) \right] \cos^2\vartheta \right\},$$

$$\langle \bar{q}'_{\frac{1}{2}} - \frac{1}{2} | V_{\Delta\Delta,1}^0 | \bar{q}_{\frac{3}{2}}^{\frac{3}{2}} - \frac{1}{2} \rangle = -D_{\Delta\Delta\frac{1}{3}} (1 + \cos\vartheta) \left[\left(- \frac{E_q^*}{M_\Delta} q'qA_+^*A_-^* + q'^2 \frac{E_q^*}{M_\Delta^2} - \frac{q'^2}{4} A_-^{*2} - 2q'(q' + q) \frac{qE_q^*}{M_\Delta^2} A_+^*B_+^* \right. \right. \\ \left. \left. - q'(q' - q) \frac{q}{M_\Delta} A_-^*B_+^* + \frac{E_q^*}{M_\Delta} q'(q' - 2q)B_+^*B_-^* \right. \right. \\ \left. \left. - \frac{q'}{M_\Delta^2} (q'E_q^{*2} - 2q^3)B_+^{*2} - (\frac{1}{4}q'^2 - q'q + q^2)B_-^{*2} \right) \right. \\ \left. + q' \left(\frac{E_q^*}{M_\Delta} (q' + q)A_+^*A_-^* + \frac{1}{2}q'A_-^{*2} + 2(q' + q) \frac{qE_q^*}{M_\Delta^2} A_+^*B_+^* + (q' - q) \frac{q}{M_\Delta} A_-^*B_+^* \right. \right. \\ \left. \left. + 2q \frac{E_q^*}{M_\Delta} B_+^*B_-^* + \frac{2}{M_\Delta^2} (q'E_q^{*2} - q^3)B_+^{*2} - (\frac{1}{2}q' - q)B_-^{*2} \right) \cos\vartheta \right. \\ \left. - q'^2 \left(\frac{1}{4}(A_-^{*2} + B_-^{*2}) + \frac{E_q^{*2}}{M_\Delta^2} (A_+^{*2} + B_+^{*2}) + \frac{E_q^*}{M_\Delta} (A_+^*A_-^* + B_+^*B_-^*) \right) \cos^2\vartheta \right].$$

Further matrix elements can be obtained by noting that

$$\langle \tilde{q}'_{\frac{1}{2}\frac{1}{2}} | V_{\Delta\Delta,1}^{\rho} | \tilde{q}\Lambda_2\Lambda_1 \rangle = \begin{cases} \langle \tilde{q}'_{\frac{1}{2}\frac{1}{2}} | V_{\Delta\Delta,1}^{\rho} | \tilde{q}\Lambda_1\Lambda_2 \rangle, & |\Lambda_1 - \Lambda_2| \text{ even} \\ -\langle \tilde{q}'_{\frac{1}{2}\frac{1}{2}} | V_{\Delta\Delta,1}^{\rho} | \tilde{q}\Lambda_1\Lambda_2 \rangle, & |\Lambda_1 - \Lambda_2| \text{ odd} \end{cases}$$

and

$$\langle \tilde{q}'_{\frac{1}{2}} - \frac{1}{2} | V_{\Delta\Delta,1}^{\rho} | \tilde{q}\Lambda_1\Lambda_2 \rangle = \langle \tilde{q}'_{\frac{1}{2}} - \frac{1}{2} | V_{\Delta\Delta,1}^{\rho} | \tilde{q} - \Lambda_2 - \Lambda_1 \rangle.$$

In addition, $\langle \tilde{q}'_{\frac{1}{2}\frac{1}{2}} | V_{\Delta\Delta,1}^{\rho} | \tilde{q} - \Lambda_1 - \Lambda_2 \rangle$ can be obtained from $-\langle \tilde{q}'_{\frac{1}{2}\frac{1}{2}} | V_{\Delta\Delta,1}^{\rho} | \tilde{q}\Lambda_1\Lambda_2 \rangle$ by replacing there $(q, \cos\vartheta)$ by $(-q, -\cos\vartheta)$ and $\langle \tilde{q}'_{\frac{1}{2}} - \frac{1}{2} | V_{\Delta\Delta,1}^{\rho} | \tilde{q} - \Lambda_1 - \Lambda_2 \rangle$ can be obtained from $\langle \tilde{q}'_{\frac{1}{2}} - \frac{1}{2} | V_{\Delta\Delta,1}^{\rho} | \tilde{q}\Lambda_1\Lambda_2 \rangle$ by the same replacement.

In actual calculations, we need the partial wave amplitudes. They are given by the general formula

$$\begin{aligned} \langle \Lambda'_1\Lambda'_2 | V^J(q', q | z) \Lambda_1\Lambda_2 \rangle \\ = 2\pi \int_{-1}^{+1} d(\cos\vartheta) d_{\Lambda\Lambda'}^J(\vartheta) \langle \tilde{q}'\Lambda'_1\Lambda'_2 | V(z) | \tilde{q}\Lambda_1\Lambda_2 \rangle, \end{aligned}$$

$$\Lambda = \Lambda_1 - \Lambda_2, \Lambda' = \Lambda'_1 - \Lambda'_2$$

and are evaluated numerically.

*Supported in part by Deutsche Forschungsgemeinschaft.

†On leave of absence at the Physics Department, SUNY at Stony Brook, Stony Brook, New York 11794.

‡Also: Institut für Theoretische Kernphysik der Universität Bonn, D-5300 Bonn, West Germany.

¹See, e.g., A. M. Green, Rep. Prog. Phys. **39**, 1109 (1976).

²K. Holinde, R. Machleidt, A. Faessler, and H. Müther, Phys. Rev. C **15**, 1432 (1977).

³P. U. Sauer, private communication.

⁴See, e.g., J. W. Durso, A. D. Jackson, and B. J. Verwest, Nucl. Phys. **A252**, 404 (1977).

⁵H. Arenhövel and W. Fabian, Nucl. Phys. **A282**, 397 (1977); E. L. Lomon, Phys. Lett. **68B**, 419 (1977).

⁶K. Holinde and R. Machleidt, Nucl. Phys. **A256**, 479, 497 (1976).

⁷R. V. Reid, Ann. Phys. (N.Y.) **50**, 411 (1968).

⁸E.g., A. M. Green and J. A. Niskanen, Nucl. Phys. **A249**, 493 (1975).

⁹K. Holinde and R. Machleidt, Nucl. Phys. **A280**, 429 (1977).

¹⁰K. Holinde and R. Machleidt, in Proceedings of the International Conference on the Nucleon-Nucleon Inter-

action, Vancouver, 1977 (unpublished).

¹¹R. A. Smith and V. R. Pandharipande, Nucl. Phys. **A256**, 327 (1976).

¹²M. Saarela, thesis, University of Oulu, Finland (unpublished).

¹³D. Schütte, Nucl. Phys. **A221**, 450 (1974).

¹⁴K. Kotthoff, K. Holinde, R. Machleidt, and D. Schütte, Nucl. Phys. **A242**, 429 (1975); K. Kotthoff, R. Machleidt, and D. Schütte, *ibid.* **A264**, 484 (1976).

¹⁵J. W. Durso, M. Saarela, G. E. Brown, and A. D. Jackson, Nucl. Phys. **A278**, 445 (1977).

¹⁶K. Erkelenz, Phys. Rep. **13C**, 191 (1974).

¹⁷G. Höhler, H. P. Jacob, and R. Strauss, Nucl. Phys. **B39**, 237 (1972).

¹⁸G. Höhler and E. Pietarinen, Nucl. Phys. **B95**, 210 (1975).

¹⁹M. MacGregor, R. Arndt, and R. Wright, Phys. Rev. **182**, 1714 (1969).

²⁰M. R. Anastasio, A. Faessler, H. Müther, K. Holinde, and R. Machleidt, Phys. Rev. C (to be published).

²¹E. Lomon, in Proceedings of the International Conference on the Nucleon-Nucleon Interaction, Vancouver, 1977 (see Ref. 10).